Constraining models of Active Galactic Nuclei: evolution of radio galaxies and the size of the narrow-line region[1]

(Fundação para a Ciência e a Tecnologia — Programa ESO; PESO/P/PRO/15133/1999)

Internal Report (CCM) nr. 42/01

Annual Report of Progress - Detailed description of scientific work

CCM, Funchal

Pedro Augusto,[1] J. Ignacio Gonzalez-Serrano,[2] Nectaria A. B. Gizani,[1] Alastair C. Edge,[3] and Ismael Perez-Fournon,[4]

[1]Centro de Ciências Matemáticas, Universidade da Madeira, Caminho da Penteada, 9050 Funchal, Portugal

[2]Instituto de Física de Cantabria (CSIC-Universidad de Cantabria), Facultad de Ciencias, 39005 Santander, Spain

[3]Dep. of Physics, University of Durham, South Road, Durham DH1 3CE, UK

[4]Instituto de Astrofísica de Canarias, c/ Via Láctea s/n, 38200 La Laguna, Tenerife, Spain

January 2001

[1]Dr. Pedro Augusto acknowledges support for this research by the European Commission under contract ERBFMGECT950012.

Abstract

We review and present the activities of the project during 2000 and those planned for 2001. We plan three lines of approach to study a sample of 55 kpc-scale radio sources (roughly half compact-medium symmetric object candidates and the other half core-plus-one-sided-jets): i) radio; ii) optical; iii) X-ray. The latter is likely to become only relevant after the project has formally finished. As regards the optical, we have concluded the first phase: BVRI photometry of $\sim$ 90% of the sample. Detailed analysis and results are progressing. We plan to follow up spectroscopically about 35 sources which lack such information and also many from the parent sample (as control sources); we also plan imaging at IR wavelengths. In the radio band, we concentrate on two main areas: detailed morphology of the sources (core finding and high resolution dual-frequency mapping) and spectra variability. The latter will be achieved from literature and catalogues searches while the former through MERLIN and VLA 22 GHz and VLBA 1.4/5 GHz observations for which we were awarded time recently. We expect to successfully conclude most of the objectives proposed within this 2 year project.

Contents

1 Introduction **3**

2 The radio side **6**

2.1 The radio view on the 55 sources 6

2.1.1 Overview 6

2.1.2 Update on Spectra 6

2.1.3 Polarization 13

2.1.4 Spectral Index 13

2.1.5 MERLIN L-band results 19

2.1.6 FIRST (on-going survey) 24

2.2 Abell 2390 24

2.3 Hercules A (to be abandoned in 2001) 29

2.4 M87 high-z replica (B2231+359) 30

2.5 B2201+044 (new interest) 31

3 The optical side **32**

3.1 Photometry 32

3.2 Spectroscopy 36

3.3 HST 39

4 The X-ray side **45**

5 General Discussion **47**

6 Conclusions and Future Work **49**

A Spectral index values (old and new) **51**

B The sample without spectral selection **54**

C 55-source sample compactness at 5 GHz **56**

D 55-source sample variability **58**

E Searching for genuine one-sided CJs **61**

F Very inverted spectrum sources **64**

G The 100-object representatives of the parent sample (optical) **66**

H Double-double radio galaxies **69**

Chapter 1

Introduction

Although the official start date of the two-year project was 1st January 2000, there has been some collaboration of the team before (namely since submission of the project by June 1999 — (Augusto et al. 1999)). The workplan proposed in this project was as presented in Figure 5 of (Augusto et al. 1999), reproduced here in Figure 1.1, with comments on the status of tasks, as well as the number of proposals submitted/accepted (where applicable). The dropped items (italic) are justified next. Some of these were replaced by equivalent tasks (presented immediately after in bold). Others were simply taken out of the project: i) all Her A items removed were dropped because we lost the team member that was working on it (see Section 2.3); ii) all X-ray related work has been dropped (except two proposals) because we have no chance to reduce the data (or even submit proposals, in some cases); iii) we have dropped the radio/optical/X-ray alignments from the project since this would require HST and X-ray data which will not be gathered during the project time even if proposals are submitted in 2001.

A lot of activity took place in 2000 as can be seen from the 'status' column in Figure 1.1. In detail, this activity is described in this work (following sections). The team were disappointed by the lack of success in some of the proposals submitted: namely the radio follow up at L-band with the MERLIN+EVN of the remaining candidates and the optical spectroscopy follow up of about two-thirds of the sample (sources that need a redshift). For every rejected proposal we will carry on with what we have been doing: review it before immediate resubmission, carefully following the referee comments, when useful. The hopes are that in the future we will get the data we need to complete the project as initially intended. In the case of the MERLIN+EVN we have decided to give up applying for it and apply for the VLBA 1.4/5 GHz instead (Figure 1.1). The success of this change was (almost) immediate.

Given all of the above, some revision of the work plan had to take place and we present the current 2001 plan in Figure 1.2, where we have dropped from Figure 1.1 all the 'done/off' tasks and transferred some undone tasks to their proper quadrimester in 2001.

			I. P-F.	A. E.	N. G.	I. G-S.	P. A.		Prop. total	Prop. acc.	Status
			×	×	×	×	×	*55 sources: EVN+MERLIN 1.6 GHz prop. subm. (CSO/MSOs)*	3	1	*off*
			×	×	×	×	×	**55 sources: VLBA 1.4/5 GHz prop. subm. (CSO/MSOs)**	2	1	**on**
			×	×	×	×	×	*55 sources: EVN+MERLIN 1.6 GHz prop. subm. (NLR probes)*	1	0	*off*
			×	×	×	×	×	**55 sources: VLBA 1.4/5 GHz prop. subm. (NLR probes)**	1	0	**later**
					×		×	55 sources: MERLIN 1.6 GHz observations of largest 12 sources			done
			×	×	×	×	×	55 sources: MERLIN 22 GHz prop. subm. (small CSO/MSOs)	3	1	on
			×	×	×	×	×	55 sources: VLA 74 MHz prop. subm.	1	0	later
	Q		×			×	×	55 sources (+ B2231): BVRI photometry observations of 20 sources			done
	1		×	×	×	×	×	55 sources: BVRI photometry proposal for remaining 30 sources	1	0	almost
			×	×	×	×	×	55 sources: optical spectroscopy proposal for 35 sources	2	0	on
				×			×	B2151+174: VLA HI absorption observations			done
					×			Her A: MERLIN+EVN 1.6 GHz observations (core region)			done
					×			*Her A: produce VLA alpha map (74 - 8400 MHz)*			*off*
				×	×		×	*Her A: XMM prop. subm.*			*off*
					×		×	55 sources: reduce MERLIN 1.6 GHz data of 12 sources			done
			×	×	×	×	×	*55 sources: single-dish 30 MHz proposal*			*off*
	Q		×	×	×	×	×	*55 sources: single-dish 100 MHz proposal*			*off*
			×	×	×	×	×	**55 sources: single-dish 30-100 MHz proposal**			**on**
	2				×		×	*55 sources: reduce single-dish 30 MHz data*			*off*
					×		×	*55 sources: reduce single-dish 100 MHz data*			*off*
			×	×	×	×	×	**55 sources: reduce single-dish 30-100 MHz data**			**later**
				×			×	B2151+174: reduce VLA HI data			done
					×		×	Her A: reduce MERLIN+EVN 1.6 GHz data (core region)			done
			×	×	×	×	×	55 sources: VLBA prop. subm. (polarization)	1	0	later*
			×	×	×	×	×	55 sources: VLA-A 22 GHz prop. subm. (NLR probes + large CSO/MSOs)	1	1	done**
					×		×	55 sources: reduce MERLIN 22 GHz (small CSO/MSOs)			later
	Q				×		×	55 sources: reduce VLA 74 MHz data			later
	3					×	×	55 sources (+B2231): reduce optical photometric data			done
						×	×	55 sources (+B2231): reduce spectroscopic data: 36 sources (redshifts)			later
			×	×	×	×	×	55 sources: what are their optical hosts?			almost
				×	×			*Her A: reduce XMM data*			*off*
			×	×	×	×	×	*55 sources: MERLIN+EVN 5 GHz prop. subm. for a few sources?*			*off****
					×		×	55 sources: reduce EVN+MERLIN 1.6 GHz (+ production of alpha maps)			almost
			×	×	×	×	×	55 sources: ASTRO-E, AXAF, XMM proposals subm.			later
				×	×		×	*55 sources (+B2231): reduce AXAF/ASTRO-E/XMM data?*			*off*
	Q			×	×		×	B2151+174: X-ray/radio correlation?			earlier
	4		×	×	×	×	×	*Her A: AXAF prop. subm.*			*off*
				×	×			*Her A: reduce AXAF data?*			*off*
					×			*Her A: model magnetic field*			*off*
					×			*Her A: model jets (ring features)*			*off*
			×	×	×	×	×	B2231+359: MERLIN+EVN 1.6+5 GHz prop. (long track if high-z)			later
					×		×	55sources: reduce the VLBA polarization data			later
					×		×	55 sources: reduce VLA 22 GHz data			on**
	Q			×	×		×	55 sources: magnetic field lines from polarizations			later
	5		×	×	×	×	×	55 sources: overall spectra and conclusions			later
			×	×	×	×	×	55 sources: get physics/ages from radio data			later
			×	×	×	×	×	55 sources: HST prop. (inspect radio/optical correlation)			on
			×	×	×	×	×	B2151+174: global picture from multi-wavelength data			earlier
			×	×	×	×	×	*55 sources: check for radio/optical/X-ray alignments*			*off*
			×	×	×	×	×	*55 sources: calculate physics from X-ray data*			*off*
	Q		×	×	×	×	×	55 sources: cosmological tests with the sample			later
	6				×		×	B2231+359: reduce EVN+MERLIN 1.6 + 5 GHz data?			later
				×	×		×	B2231+359: get core + knot composite spectra			later
			×	×	×	×	×	B2231+359: is it really an M87 replica at high-z?			later
			×	×	×	×	×	Global conclusions and final assessments - teminate papers			later

Figure 1.1: The updated workplan adapted from (Augusto et al. 1999). Notes: * VLBA: 1.4/5 GHz + polarization; ** VLA-BnA observations of some CSO/MSOs only — NLR probes cannot be done during this project since the next VLA-A configuration is in 2 yrs; *** we have dual 1.4/5 GHz VLBA time awarded, which should do the job.

			I.-P.F.	A. E.	I.-G.-S.	P. A.		Prop. total	Prop. acc.	Status
			×	×	×	×	55 sources: VLBA 1.4/5 GHz prop. subm. (CSO/MSOs)	2	1	on
			×	×	×	×	55 sources: MERLIN 22 GHz prop. subm. (small CSO/MSOs)	3	1	on
			×	×	×	×	55 sources: BVRI photometry proposal for remaining 30 sources	1	0	almost
	Q		×	×	×	×	55 sources: near-IR photometry proposal for all	1	0	on
	1		×	×	×	×	55 sources: optical spectroscopy proposal for 35 sources	2	0	on
			×	×	×	×	55 sources: what are their optical hosts?			almost
						×	55 sources: reduce EVN+MERLIN 1.6 GHz (+ production of alpha maps)			almost
				×		×	B2151+174 paper: X-ray/radio correlation? Global picture			on
			×	×	×	×	55 sources: VLBA 1.4/5 GHz prop. subm. (NLR probes)	1	0	
	Q					×	55 sources: reduce VLA 22 GHz data			on**
	2		×	×	×	×	55 sources: Chandra proposals subm. for the best			
					×	×	55 sources (+B2231): reduce spectroscopic data: 36 sources (redshifts)			
			×	×	×	×	55 sources: HST prop. (inspect radio/optical correlation)			on
			×	×	×	×	55 sources: get physics/ages from radio data			
			×	×	×	×	B2231+359: MERLIN+EVN 1.6+5 GHz prop. (long track if high-z)			
						×	55 sources: reduce MERLIN 22 GHz (small CSO/MSOs)			
			×	×	×	×	55 sources: VLBA prop. subm. (polarization)	1	0	*
						×	55sources: reduce the VLBA polarization data			
			×	×	×	×	55 sources: single-dish 30-100 MHz proposal			
			×	×	×	×	55 sources: cosmological tests with the sample			
	Q		×	×	×	×	55 sources: VLA 74 MHz prop. subm.	1	0	
	3					×	B2231+359: reduce EVN+MERLIN 1.6 + 5 GHz data?			
				×		×	B2231+359: get core + knot composite spectra			
			×	×	×	×	B2231+359: is it really an M87 replica at high-z?			
						×	55 sources: reduce single-dish 30-100 MHz data			
			×	×	×	×	55 sources: XMM proposals subm. for the best			
				×		×	55 sources: magnetic field lines from polarizations			
						×	55 sources: reduce VLA 74 MHz data			
			×	×	×	×	55 sources: overall spectra and conclusions			
			×	×	×	×	Global conclusions and final assessments - terminate papers			

Figure 1.2: The updated workplan adapted from (Augusto et al. 1999). Notes: * VLBA: 1.4/5 GHz + polarization; ** VLA-BnA observations of some CSO/MSOs only — NLR probes cannot be done during this project since the next VLA-A configuration is in 2 yrs.

Chapter 2

The radio side

2.1 The radio view on the 55 sources

2.1.1 Overview

To show the progress that has been made by the team submission of the project in June 99 (Augusto et al. 1999), we update Table 1 of the Scientific case of that document. The revised Table is presented in Table 2.1 here where we see that almost half of the sample (∼24 objects out of 53) have high resolution spectral index maps ($\alpha^5_{1.6}$) available ($\surd$) or ready for production since the data exists ('Pot'), in two cases these are in the literature ('Lit/Pot'). One of the aims of our project is to produce spectral index maps for all sources, that is, to clear the 29 '—' that exist in Column (7) of Table 2.1. For most of the CSO/MSOs remaning (and some NLR probes), we will have VLBA 1.4/5 GHz data available.

2.1.2 Update on Spectra

Since the spectra of the 55 candidates have been published (Augusto et al. 1998), new radio surveys have come up with results and many include flux densities of our sources in their lists (at different frequencies). Also, the Nasa Extragalactic Database (NED) got updated as regards source flux densities in quite old references. Other data (e.g. 4850 MHz) were revised in new catalogues — GB6 (Gregory et al. 1996) vs. (Gregory & Condon 1991). In Figure 2.1 we update the spectra of the 55 sources. The new references are presented in Table 2.2. The old references are in Table A1 of Augusto et al. (1998).

The team decided to pursue the part of the work plan (Augusto et al. 1999) that aims at finding the fluxes at $\sim$ 100 MHz of all candidates since the vast majority still has a yet to determine turnover frequency in their overall spectra. We applied once to VLA 74 MHz time and got rejected with the argument that the turnover determination could wait for all the rest of the work within the project. We agreed to drop the VLA possibility, at least until we have single dish observations at 30–100 MHz. There are hopes of collaboration with russian scientists (Puschino Observatory) and the PI will have meetings there in June 2001 with such purpose. We might find that for many sources it would be more suitable to use e.g. the GMRT interferometer at 150 MHz which is less limited by confusion with a resolution of about 1

Table 2.1: Augusto et al. (1998) 23 CSO/MSO candidates (top) and 30 NLR probes (bottom) — the radio follow-up 'board'. The remaining two objects of the 55-source sample are a 'lens' and a large object. Description: **(1)** The candidate name in B1950.0; * redshift data exist; † this might be a CSO/MSO — Figure 2.4; **(2)** distinction, from their angular sizes (independent of z), between: i) CSO/MSO; ii) In(ner)/Bo(rder) NLR probes; for (MSO) and (Bo NLR): $z > 0.2$ was assumed — (Augusto et al. 1999); **(3),(4)** Current status of L-band follow-up; **(5),(6)** Current status of C-band follow-up; **(7)** Spectral index map: $\surd$—map has been made; 'Pot'—data exist to make map; 'Lit/Pot'—data exist in the literature; **(8)** Current status of K-band core searches.

CSO/MSO	Type	L-band		C-band		$\alpha^5_{1.6}$ map	22 GHz
candidates	($z > 0.2$)	MERLIN+EVN	MERLIN	MERLIN	VLBA		MERLIN/VLA
(1)	**(2)**	**(3)**	**(4)**	**(5)**	**(6)**	**(7)**	**(8)**
B0046+316*	MSO	literature		observed		Lit/Pot	
B0112+518	(MSO)			observed		—	
B0116+319*	CSO	literature		observed		Lit/Pot	
B0205+722*	MSO		observed	observed		Pot	
B0225+187	CSO/MSO	observed		observed	observed	$\surd$	
B0233+434	CSO			observed	observed	—	
B0352+825	CSO			observed	observed	—	observed
B0638+357	(MSO)	observed		observed		$\surd$	
B0732+237	CSO	observed		observed	observed	$\surd$	observed
B0817+710	CSO/MSO			observed	observed	—	
B0819+082	CSO/MSO	observed		observed		$\surd$	
B0824+355*	MSO		observed	observed		Pot	
B1010+287	CSO			observed	observed	—	
B1058+245	(MSO)			observed		—	
B1212+177	CSO			observed	observed	—	
B1233+539	CSO/MSO			observed		—	
B1504+105	CSO			observed	observed	—	
B1628+216	(MSO)			observed		—	
B1801+036	(MSO)			observed		—	observed
B1928+681	CSO			observed	observed	—	observed
B1947+677	(MSO)			observed	literature	—	
B2151+174*	CSO	observed		observed	observed	$\surd$	
B2345+113	CSO/MSO	observed		observed		Pot	

NLR	Type	L-band		C-band		$\alpha^5_{1.6}$ map	22 GHz
probes	($z > 0.2$)	MERLIN+EVN	MERLIN	MERLIN	VLBA		MERLIN/VLA
(1)	**(2)**	**(3)**	**(4)**	**(5)**	**(6)**	**(7)**	**(8)**
B0127+145	(Bo NLR)	observed		observed		$\surd$	
B0345+085	In/Bo NLR	observed		observed		$\surd$	
B0351+390	(Bo NLR)		observed	observed		Pot	
B0418+148	(Bo NLR)			observed		—	
B0429+174	(Bo NLR)		observed	observed		Pot	
B0529+013	(Bo NLR)	observed		observed		$\surd$	
B0821+394*	Bo NLR		observed	observed		Pot	
B0905+420*	Bo NLR			observed		—	
B0916+718*	Bo NLR		observed	observed		Pot	
B1003+174	(Bo NLR)			observed		—	
B1011+496*	Bo NLR		observed	observed		Pot	
B1143+446*	Bo NLR			observed		—	
B1150+095*	Bo NLR			observed		—	
B1211+334*	Bo NLR			observed	observed	—	observed
B1241+735*	Bo NLR		observed	observed		Pot	
B1317+199	(Bo NLR)			observed		—	
B1342+341	(Bo NLR)			observed		—	
B1638+124*	Bo NLR			observed		—	
B1642+054	(Bo NLR)		observed	observed		Pot	
B1722+562	(Bo NLR)		observed	observed		Pot	
B1744+260*	In NLR			observed		—	observed
B1812+412*	Bo NLR			observed		—	
B1857+630	In/Bo NLR			observed	observed	—	observed
B2101+664†	*In/Bo NLR*		*observed*	*observed*		*Pot*	
B2112+312	In/Bo NLR			observed		—	
B2150+124	(Bo NLR)		observed	observed		Pot	
B2201+044*	Bo NLR			observed		—	
B2205+389	(Bo NLR)			observed		—	
B2210+085	(Bo NLR)	observed		observed		$\surd$	
B2247+140*	In NLR			observed		—	

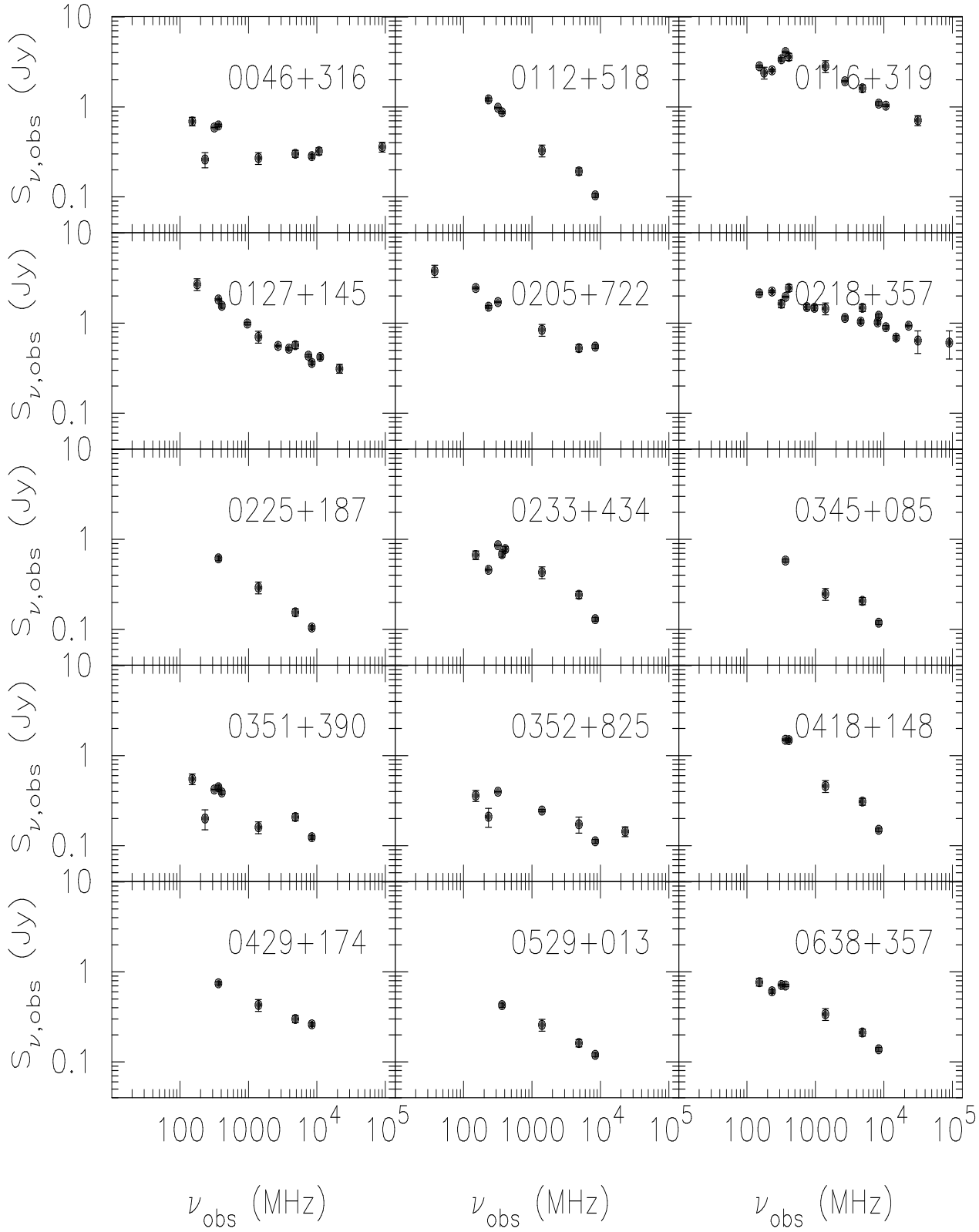
0046+316
0112+518
0116+319
0127+145
0205+722
0218+357
0225+187
0233+434
0345+085
0351+390
0352+825
0418+148
0429+174
0529+013
0638+357
$S_{\nu,obs}$ (Jy)
10
1
0.1
100 1000 10^4 10^5
ν_{obs} (MHz)

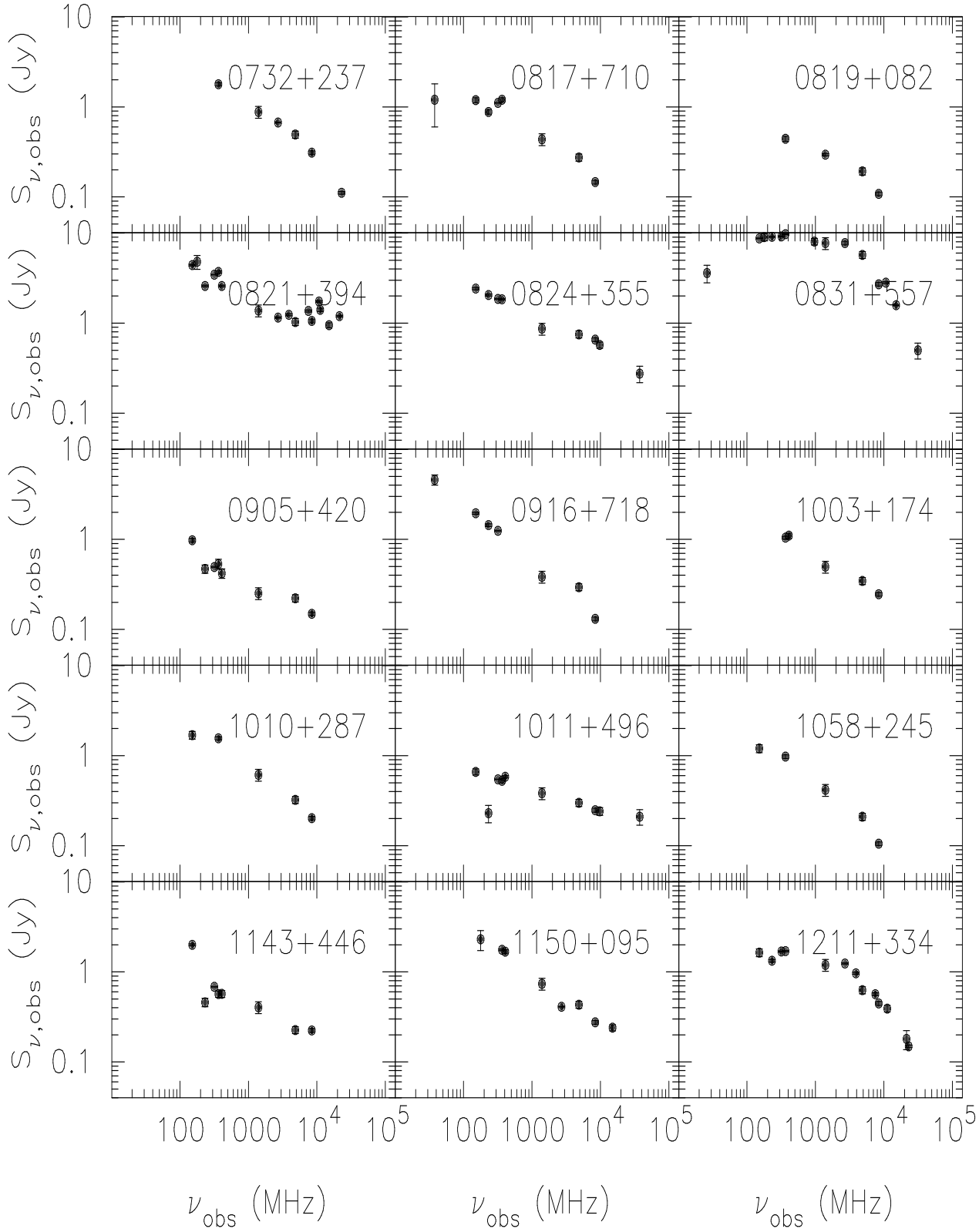
0732+237
0817+710
0819+082
0821+394
0824+355
0831+557
0905+420
0916+718
1003+174
1010+287
1011+496
1058+245
1143+446
1150+095
1211+334
10
1
0.1
100 1000 10^4 10^5
$S_{\nu,obs}$ (Jy)
ν_{obs} (MHz)

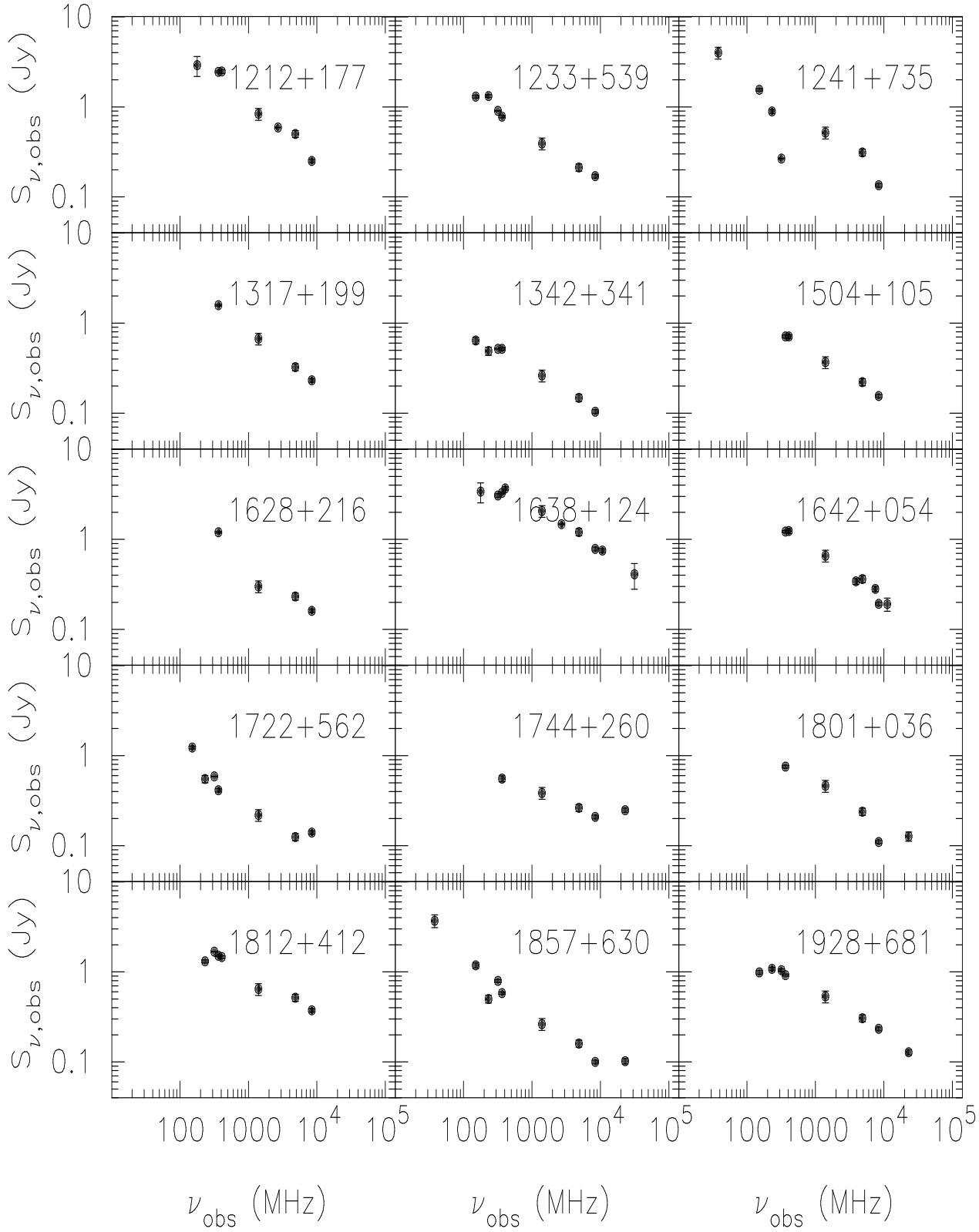
1212+177
1233+539
1241+735
1317+199
1342+341
1504+105
1628+216
1638+124
1642+054
1722+562
1744+260
1801+036
1812+412
1857+630
1928+681
10
1
0.1
100 1000 10^4 10^5
S_ν,obs (Jy)
ν_obs (MHz)

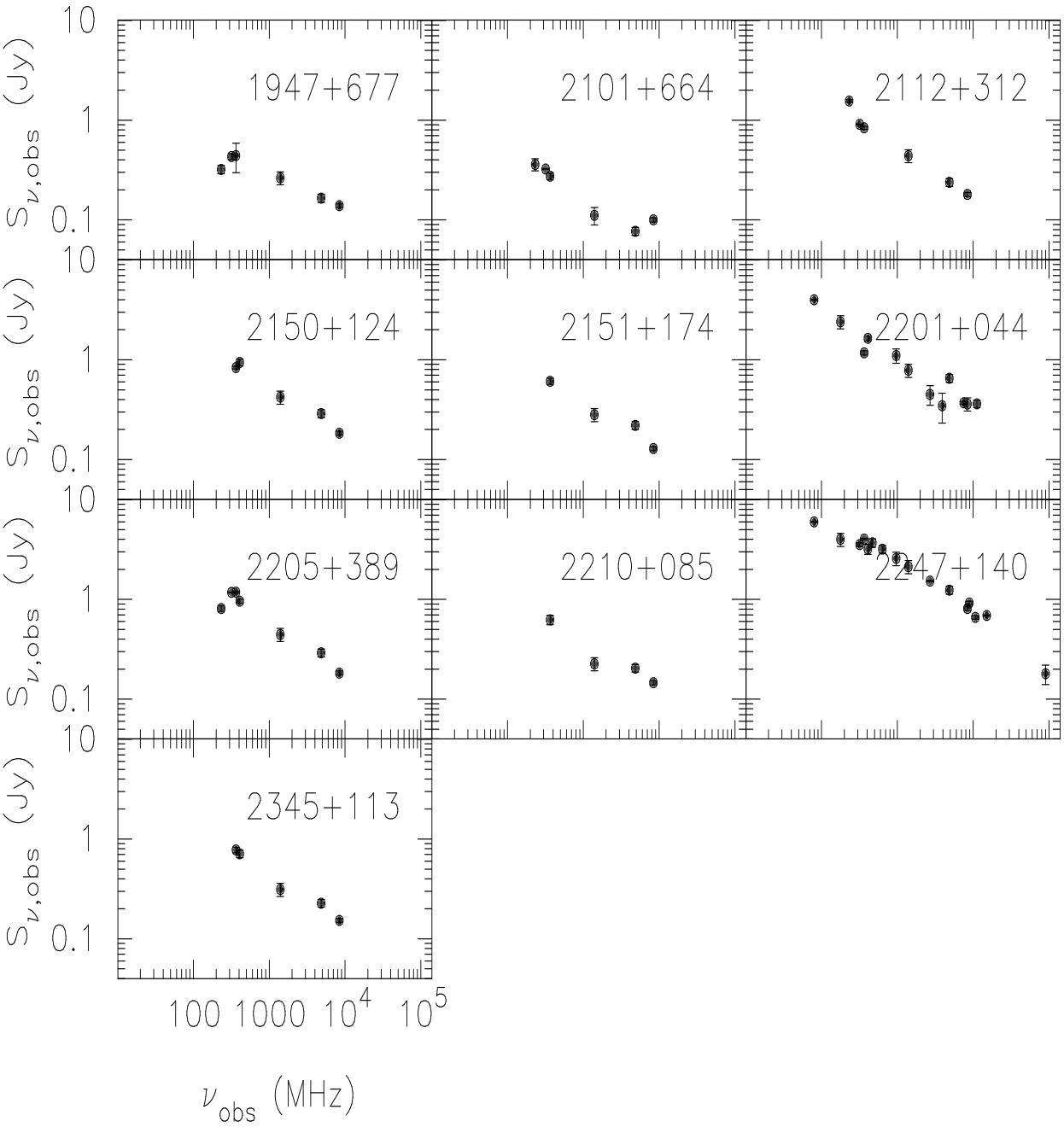

Figure 2.1: The spectra of the 55 sources — see Table 2.2 for references. Some of the 232 MHz data points that come from (Zhang et al. 1997) are actually lower limits, since they correspond to peak flux densities. These are for the sources: B0046+316, B0112+518, B0116+319, B0205+722, B0218+357, B0233+434, B0351+390, B0352+825, B0817+710, B0905+420, B0916+718, B1011+496, B1143+446, B1211+334, B1342+341, B1812+412, B2101+664, B2112+312, B2205+389.

Table 2.2: The new references for the spectra update of the 55 sources presented in Figure 2.1 (as well as B2231+359 — Figure 2.10). Frequencies are approximated, for simplicity (for synchrotron model fitting, actual frequency values will be used): e.g. 318 MHz for WENSS which is actually at 326 MHz.

Freq. (MHz)	Ref.	Freq. (MHz)	Ref.	Freq. (MHz)	Ref.
26	1	635	1	8900	14
38	2	750	1	10700	15
80	3	966	9, 10	11200	10
151	4	2700	3, 8, 9	15000	16, 17
178	1, 5	3900	9, 10	21400	10
232	6	4585	11	23000	18, 19
318	7	4850	12	31400	20
408	3,8	7500	10	90000	21
468	1	8100	13		

[1] (Kühr et al. 1981)
[2] (Rees 1990)
[3] Parkes Catalogue (1990), published by the Australia Telescope National Facility
[4] (Waldram et al. 1996)
[5] (Gower et al. 1965)
[6] (Zhang et al. 1997)
[7] (Rengelink et al. 1997)
[8] (Large et al. 1981)
[9] (Bursov 1997)
[10] (Kovalev et al. 1999)
[11] (Owen et al. 1978)
[12] (Gregory et al. 1996)
[13] (Owen et al. 1980)
[14] (Shimmins & Wall 1973)
[15] (Gregorini et al. 1998)
[16] (Genzel et al. 1976)
[17] (Spencer et al. 1989)
[18] Our data and (Augusto et al. 1998)
[19] (Patnaik et al. 1993)
[20] (Geldzahler & Witzel 1981)
[21] (Joyce & Simon 1976)

arcmin.

2.1.3 Polarization

(Augusto et al. 1998) have presented the 55-source sample 8.4 GHz polarizations which are, in general, quite low, at an average of 2% (their Figure 5). However, the two main populations of radio sources (CSO/MSOs and CJs) have different distributions, with the CJs more polarized than the CSO/MSOs (Figure 8 in (Augusto et al. 1998)). This means that, for the understanding of our sample and their two radio populations, the study of their radio polarizations is important. The plan of carrying out this study was already in the workplan of (Augusto et al. 1999). Given that we are planning to follow up at L-band with higher resolution all objects (half done — see Table 2.1) and the EVN, currently, has no great polarization measurement capabilities, the VLBA seems to be the ideal array to apply for time in the future since: i) the resolution is better; ii) can perform imaging and polarization at the same epoch, even at two or more different frequencies, if necessary (impossible with the EVN) — spectral index maps in real time; iii) might show us the way out of the proposal rejection cycle that we have entered with the EVN. In fact, very recently (Jan 2001) we had success with VLBA dual frequency observations (but not yet with polarization), which should be done later.

Polarization information will enable us to learn about the magnetic fields and shocks in the sources and may lead to a better physical insight into what is actually going on in the 55 sources, tying up their multi-wavelength properties. Shock evidence is particularly important for the 'NLR probes', which should also so shocks in their optical spectra.

2.1.4 Spectral Index

We are planning to construct high resolution spectral index maps for the whole sample. Since we already have MERLIN 5 GHz data for all sources available (some even MERLIN + VLBA 5 GHz), we need 1.6 GHz data, with MERLIN for the largest sources and with EVN+MERLIN or VLBA alone for the smallest. In Table 2.1 we see that nine spectral index maps have been produced while fifteen more await reduction: almost half of the sample is 'done'. We plan to do the remaining with the VLBA (as well as polarization). For similar sources, 'repeated' multi-epoch data (different epoch MERLIN+EVN and VLBA) would be useful for velocity/ages determinations for our CSO/MSO candidates, and for eventual detection of superluminal motions in 'NLR probes'. In what follows, we consider source variability issues.

(Augusto et al. 1998) in their Figure 6 have shown that the spectral index distribution of the 55-source sample is biased towards the highest values possible (within flatness: $\alpha_{1.4}^{4.85} < 0.5$; $S_\nu \propto \nu^{-\alpha}$) as compared to the parent sample from where the 55 kpc-scale sources were selected. This can more easily be explained by a correlation between radio structure and a high value of the spectral index.

Several issues remain open, however. One of these has to do with the variability of the radio sources: (Augusto et al. 1998) have used catalogues at 1.4 GHz (White & Becker 1992) and at 4.85 GHz (Gregory & Condon 1991) that have now been superseeded (NVSS — (Condon et al. 1998) and GB6 — (Gregory et al. 1996), respectively). The first update is more relevant than the second, since it is a completely new survey, conducted about 10 yrs later than the

Table 2.3: The eleven CSO/MSOs and the four CJs of the 55-source sample that would be out of the sample if the $\alpha_{1.4}^{4.85} < 0.5$ criterion was used with the most recent catalogues (Condon et al. 1998; Gregory et al. 1996) — 'new' — rather than with the oldest (White & Becker 1992; Gregory & Condon 1991) — 'old' — as was the case in (Augusto et al. 1998). See Appendix A for a full list for the 55-source sample.

CSO/MSOs	$\alpha_{1.4}^{4.85}$ (old)	$\alpha_{1.4}^{4.85}$ (new)	CJs	$\alpha_{1.4}^{4.85}$ (old)	$\alpha_{1.4}^{4.85}$ (new)
B0112+518	0.37	0.68	B1150+095	0.31	0.51
B0225+187	0.48	0.51	B1211+334	0.49	0.65
B0233+434	0.45	0.60	B1317+199	0.45	0.65
B0732+237	0.37	0.51	B2205+389	0.33	0.52
B0817+710	0.37	0.63			
B1010+287	0.49	0.55			
B1058+245	0.47	0.63			
B1212+177	0.24	0.57			
B1233+539	0.48	0.62			
B1628+216	0.16	0.63			
B1928+681	0.41	0.51			

first one. The 4.85 GHz update was mostly an improvement in the errors of the catalogue and consequent difference in the actual mean value of the flux densities, which we use, for example, to plot spectra (c.f. Figure 2.1).

The question we tried to address first was: will the number of kpc-scale sources selected from the parent sample change significantly if, rather than using the 1.4/4.85 GHz catalogues that we did (White & Becker 1992; Gregory & Condon 1991) to calculate the $\alpha_{1.4}^{4.85}$ spectral indices we use the 1.4/4.85 GHz NVSS/GB6 catalogues? We remind here that (Augusto et al. 1998) have used the rejection criterion $\alpha_{1.4}^{4.85} < 0.5$. The answer is that 15 out of 55 sources (Table 2.3) would actually be **out** of the (Augusto et al. 1998) sample, or 27% (Appendix A). The spectral index distributions ('new' and 'old'), however, compare as in Figure 2.2 where they are the same at a 10% significance level. Hence, the $\alpha_{1.4}^{4.85}$ criterion is stable to the variability of sources as regards the statistical properties of the sample as a whole. Since the 27% fraction is a relatively large number, we must understand physically what has happened. Surely the main contribution to the difference must come from the 10 yr difference in the epochs of the 1.4 GHz catalogues, since the 4.85 GHz catalogues are the same (values taken at the same epoch). Can it be that the difference is explained alone by the secular variability of the sources?

At this point, we should note that out of the 15 sources that would be put out of the sample in the new version, 11 are CSO/MSOs (the other four beeing CJs) — Table 2.3. Could it be that these particular CSO/MSOs are ageing or getting larger and getting a steeper spectra? or is it that an overall increase in luminosity (consistent with secular variation) is taking place? Although the first explanation, given the typical ages of kpc CSO/MSOs of 10^3-10^5 yrs appears not to be good, it is possible that, if the CSO/MSOs were at the border of the $\alpha_{1.4}^{4.85}$ criterion, they would 'jump' over in 10 yrs. To check this we look at Table 2.3. We see that the behaviour is not as anticipated since not many CSO/MSOs had previous values close to the $\alpha_{1.4}^{4.85} < 0.5$

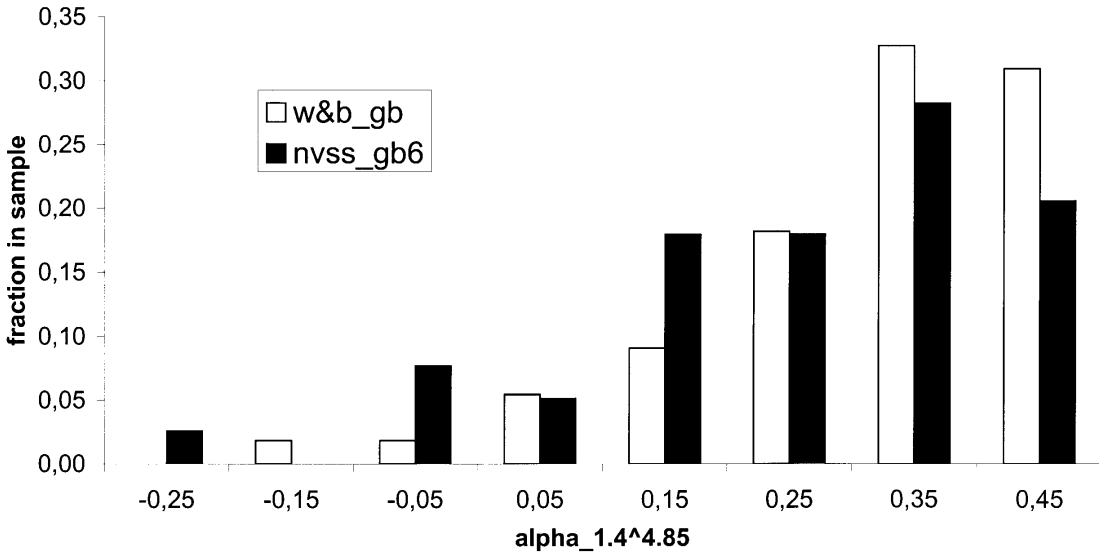

Figure 2.2: The spectral index distributions ($\alpha_{1.4}^{4.85} < 0.5$) of the 55- source sample as in (Augusto et al. 1998) — w&b_gb — and using the more recent catalogues — nvss_gb6. The latest version contains only 36 sources of the original sample since the remaining sources 'jump' over the flat-spectrum border as discussed in the text. The two distributions are the same at the 10% significance level.

border. Some are quite far (B1212+177; $\alpha_{1.4}^{4.85} = 0.24$) and still managed to jump over. Others are quite close (B0225+187; $\alpha_{1.4}^{4.85} = 0.48$) and just managed to do it. An important fact is that for *all* 11 CSO/MSOs (and also the four CJs) listed in Table 2.3 there was an increase in $\alpha_{1.4}^{4.85}$, most likely due to an increase in the 1.4 GHz flux densities (and luminosities) over 10 yrs. This is not the case for all of the remaining sources in the sample, since many had an opposite variation of $\alpha_{1.4}^{4.85}$ (Appendix A). Another explanation for the 'jump' could be that the errors in flux densities (which were not considered in Table 2.3) could be relevant, although, a priori, they seem pretty low (e.g. ∼3% at 1.4 GHz in (White & Becker 1992) for most sources). This issue needs further investigation.

We must first find out what happened to the sources that the $\alpha_{1.4}^{4.85} < 0.5$ (Augusto et al. 1998) criterion has rejected and that now, probably due to secular variability, using the NVSS flux values, could well be in the sample. We must start by emphasizing that the JVAS/CLASS, from where our parent sample was drawn, is *not* complete to all spectral indices of radio sources but it is biased to contain flat-spectrum sources (complete for $\alpha < 0.5$). From (Augusto 1996) we picked all sources that had kpc-scale structure but were rejected due to the spectral index criterion alone. They total 98 and, of these, 27 (which include 17 with $0.5 \leq \alpha_{1.4}^{4.85} \leq 0.6$) would be *inside* the (Augusto et al. 1998) kpc-scale sample, had they used NVSS and GB6 instead of (White & Becker 1992; Gregory & Condon 1991): 28% of the sources would 'jump' over to the flat spectrum side (Figure 2.3) as compared with the 27% that would make the other direction as we have seen above. Since the numbers are very similar, this seems to suggest, once again, that the spectral index criterion is quite robust statistically for our sample. In Appendix B we briefly discuss the general population of JVAS/CLASS kpc-scale sources (flat + steep). In Appendix C we compare directly the fluxes from the NVSS and the MERLIN 5 GHz flux densities of (Augusto et al. 1998) in order to get a feeling of the compactness of the objects at high frequency.

Coming back to the question of secular variability, we are currently undertaking a study in the literature of all 55 sources, looking for the explanation of the spectral index 'jumps' described above, and also because variability in a short time scale, in radio sources, helps us to gather more physical information about them, namely their sizes. Going through NED for all 55 sources, only a few had data points at different frequencies that disagree. This disagreement is defined as follows: given two fluxes with their errors $\mu_1 \pm \sigma_1$ and $\mu_2 \pm \sigma_2$, whenever a source, at a given frequency, has $(\mu_1 < \mu_2)$ $\mu_1 + \sigma_1 < \mu_2 - \sigma_2$, then it is classified as *variable* at that frequency. The list of such variable sources (21 out of 55) is presented in Table 2.4 and a more complete version in Appendix D. Several arguments will now be put forward, since this number (40% of the sample) is quite large.

First, we note from Table 2.4 that only 7 of the 'variable' sources show an α 'jump' and that many of the 21 'variable' sources do not show any extraordinary variation of $\alpha_{1.4}^{4.85}$, for example, B1010+287 (0.49 to 0.55). It is then interesting that 8 of the fifteen sources with the α 'jump' (listed in Table 2.3) are not 'variable'. Is this because there is not enough data at different epochs in the literature to judge about their variability (*no data* class) or is it because, more importantly, they are actually *non-variable* (another class) with at least a couple of different epoch literature points? This issue needs clarification to understand the meaning of 'variability' in the 55-source sample. In fact, the same question should be addressed for the 34 sources of the 55-source sample that are 'non-variable'. Are they really non-variable or are there simply not enough data to judge? It could be that 21 'variable' sources in the sample is actually a lower limit. Further work must be done on this area in the near future, since the number of

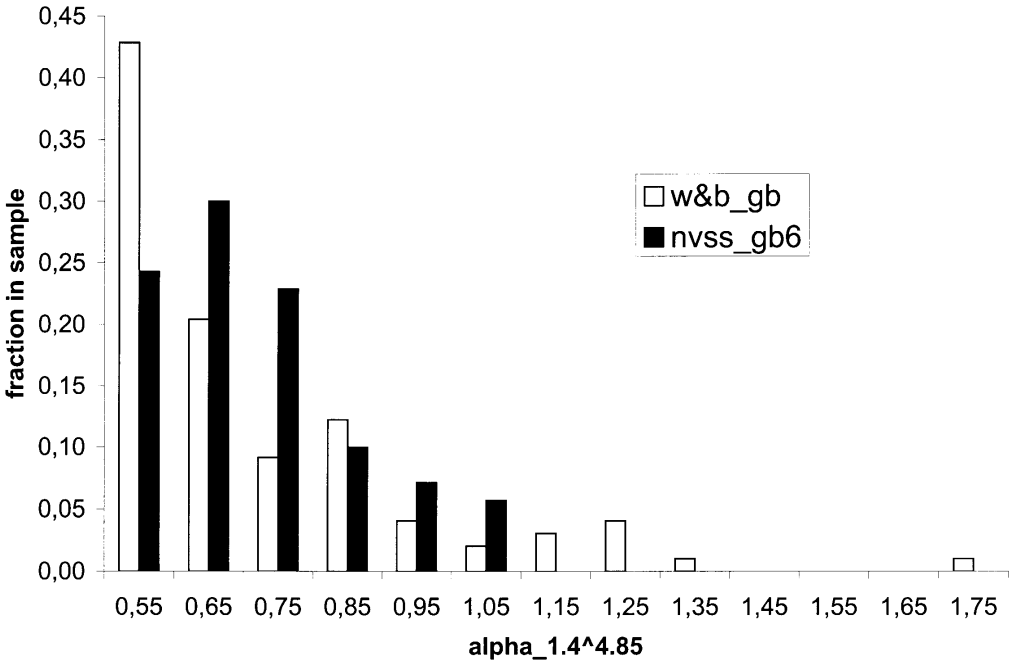

Figure 2.3: The spectral index distributions ($\alpha_{1.4}^{4.85} \geq 0.5$) of the 98 kpc-scale sources that have steep spectra and are not in the 55-source sample of (Augusto et al. 1998). The catalogues are as in Figure 2.2. The *nvss_gb6* contains only 70 sources of the original sample of 98 since the remaining 'jump' over the steep-spectrum border (to the left) as discussed in the text. The two distributions are different at the 95% confidence level. We have yet to find a suitable explanation for this, although it is a marginal question for the science we are trying to get from our 55-source sample.

Table 2.4: The 21 sources out of the 55 that 'vary', at least secularly (nine CSO/MSOs and eleven CJs). $\alpha_{1.4}^{4.85}$ values are given using the new catalogues (Condon et al. 1998; Gregory et al. 1996) and using the old (White & Becker 1992; Gregory & Condon 1991). The sources with a α 'jump' are the ones which are rejected with the new values from the 55-source sample and are also listed in Table 2.3.

Variable source	Type	$\alpha_{1.4}^{4.85}$ (old)	$\alpha_{1.4}^{4.85}$ (new)	α 'jump'
B0112+518	MSO	0.37	0.68	$\surd$
B0116+319	CSO	0.47	0.40	
B0127+145	CJ	0.22	0.25	
B0205+722	MSO	0.33	0.19	
B0218+357	lens	-0.02	0.12	
B0429+174	CJ	0.37	0.18	
B0817+710	CSO/MSO	0.37	0.63	$\surd$
B0819+082	CSO/MSO	0.30	0.35	
B0916+718	CJ	0.22	0.41	
B1010+287	CSO	0.49	0.55	$\surd$
B1211+334	CJ	0.49	0.65	$\surd$
B1212+177	CSO	0.24	0.57	$\surd$
B1241+735	CJ	0.33	-0.05	
B1628+216	MSO	0.16	0.63	$\surd$
B1638+124	CJ	0.38	0.43	
B1642+054	CJ	0.42	0.34	
B1722+562	CJ	0.41	0.38	
B1801+036	MSO	0.49	0.11	
B2201+044	CJ	0.04	-0.27	
B2205+389	CJ	0.33	0.52	$\surd$
B2210+085	CJ	0.07	0.20	

'variable' sources with an α 'jump' could increase substantially.

Second, and also important, is the determination of the type of variability seen: is it secular or burst-like? It should be possible to co?duct a first order approach by studying the time interval between epochs for all 'variable' sources. For this, we will have to?go back to the literature and fill Table D.1 with the dates of the measurements.

Third, the preliminary results of 'variable' sources in Table 2.4 suggest a rough similar number of CJs and CSO/MSOs. Given the accepted notion that CJs are more variable than CSO/MSOs in short term variability, it looks, by now, that the variability is secular and not short term for all sources that 'vary'. Surely, we must confirm the suggestion with a self-consistent 'variable' sample of sources as described above, when the *no data* class disappears.

Fourth, it might be more useful in the future to define variability as fraccional instead of the way it was defined above. For example, we could use $|\mu_1 - \mu_2| / \mu_1$ greater than a given value for variable sources (this value could be 20%, 50%, etc.). This has also the advantage of allowing us to pick sources with different degrees of variability, enhancing any hidden trends in the 55-source sample.

2.1.5 MERLIN L-band results

In Figure 2.4 we present our recent results after reducing the data of the MERLIN 1.6 GHz snapshot imaging of the 13 largest sources in our sample. Together with the existing MERLIN 5 GHz data, we will produce spectral index maps for all these sources ('Pot' in Table 2.1).

A side project emerged from these results: the search for genuine one-sided core-jet sources, since many of these 13 sources are one-sided at more than 30:1 flux density ratio. This new idea, as well as follow up prospects, are discussed in Appendix E.

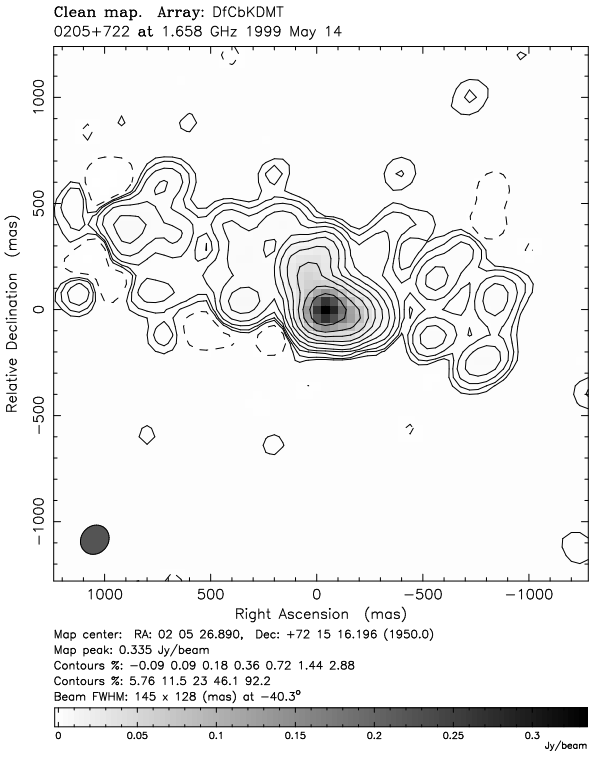
Clean map. Array: DfCbKDMT
0205+722 at 1.658 GHz 1999 May 14
Relative Declination (mas)
Right Ascension (mas)
Map center: RA: 02 05 26.890, Dec: +72 15 16.196 (1950.0)
Map peak: 0.335 Jy/beam
Contours %: −0.09 0.09 0.18 0.36 0.72 1.44 2.88
Contours %: 5.76 11.5 23 46.1 92.2
Beam FWHM: 145 x 128 (mas) at −40.3°
Jy/beam

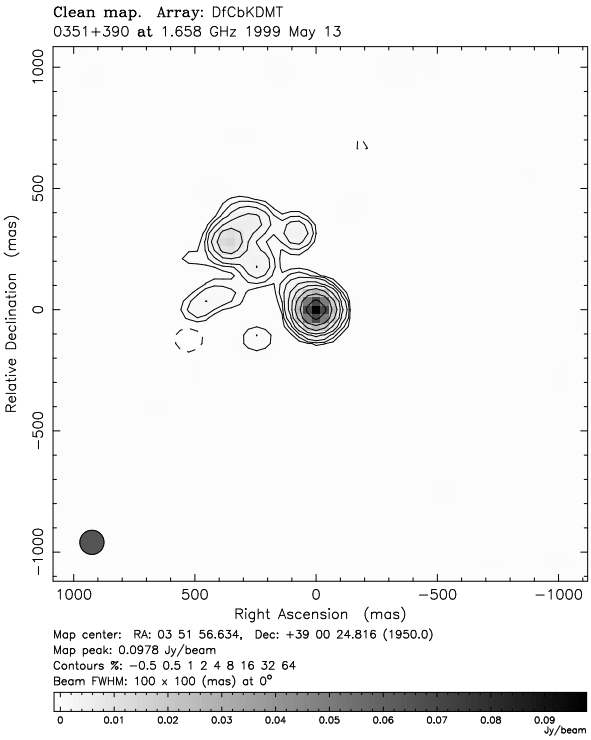
Clean map. Array: DfCbKDMT
0351+390 at 1.658 GHz 1999 May 13
Relative Declination (mas)
Right Ascension (mas)
Map center: RA: 03 51 56.634, Dec: +39 00 24.816 (1950.0)
Map peak: 0.0978 Jy/beam
Contours %: −0.5 0.5 1 2 4 8 16 32 64
Beam FWHM: 100 x 100 (mas) at 0°
Jy/beam

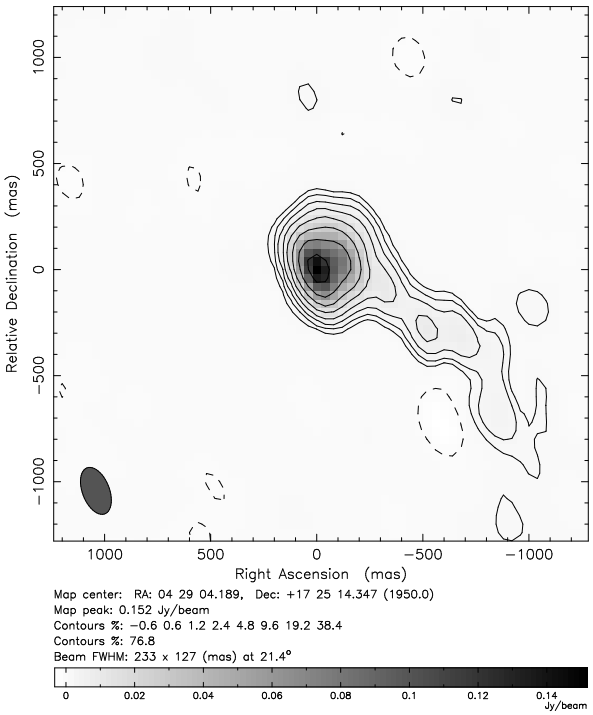
Clean map. Array: DfCbKDMT
0429+174 at 1.658 GHz 1999 May 13
Relative Declination (mas)
Right Ascension (mas)
Map center: RA: 04 29 04.189, Dec: +17 25 14.347 (1950.0)
Map peak: 0.152 Jy/beam
Contours %: −0.6 0.6 1.2 2.4 4.8 9.6 19.2 38.4
Contours %: 76.8
Beam FWHM: 233 x 127 (mas) at 21.4°
Jy/beam

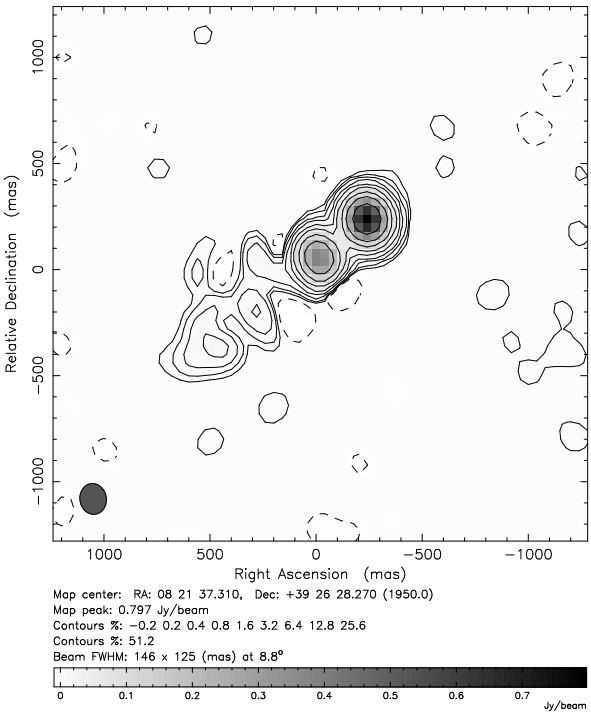
Clean map. Array: DfCbKDMT
0821+394 at 1.658 GHz 1999 May 13
Relative Declination (mas)
Right Ascension (mas)
Map center: RA: 08 21 37.310, Dec: +39 26 28.270 (1950.0)
Map peak: 0.797 Jy/beam
Contours %: −0.2 0.2 0.4 0.8 1.6 3.2 6.4 12.8 25.6
Contours %: 51.2
Beam FWHM: 146 x 125 (mas) at 8.8°
Jy/beam

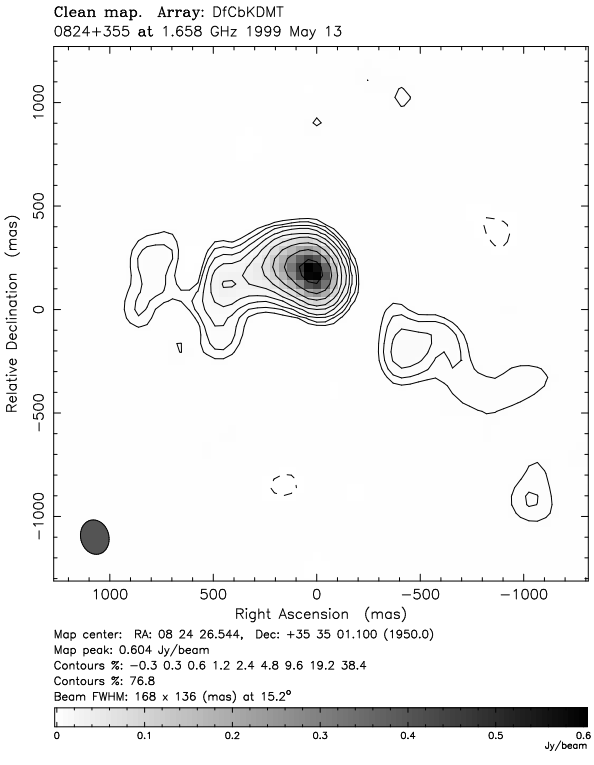
Clean map. Array: DfCbKDMT
0824+355 at 1.658 GHz 1999 May 13
Relative Declination (mas)
Right Ascension (mas)
Map center: RA: 08 24 26.544, Dec: +35 35 01.100 (1950.0)
Map peak: 0.604 Jy/beam
Contours %: −0.3 0.3 0.6 1.2 2.4 4.8 9.6 19.2 38.4
Contours %: 76.8
Beam FWHM: 168 x 136 (mas) at 15.2°
Jy/beam

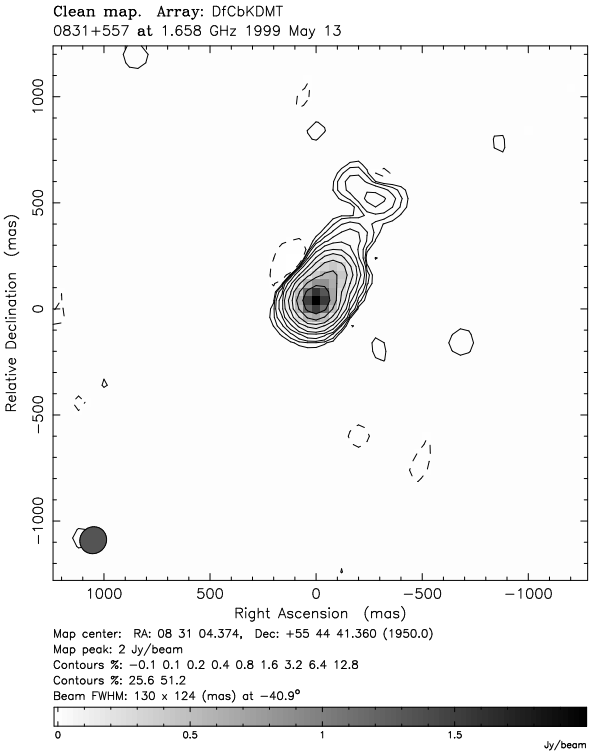
Clean map. Array: DfCbKDMT
0831+557 at 1.658 GHz 1999 May 13
Relative Declination (mas)
Right Ascension (mas)
Map center: RA: 08 31 04.374, Dec: +55 44 41.360 (1950.0)
Map peak: 2 Jy/beam
Contours %: −0.1 0.1 0.2 0.4 0.8 1.6 3.2 6.4 12.8
Contours %: 25.6 51.2
Beam FWHM: 130 x 124 (mas) at −40.9°
Jy/beam

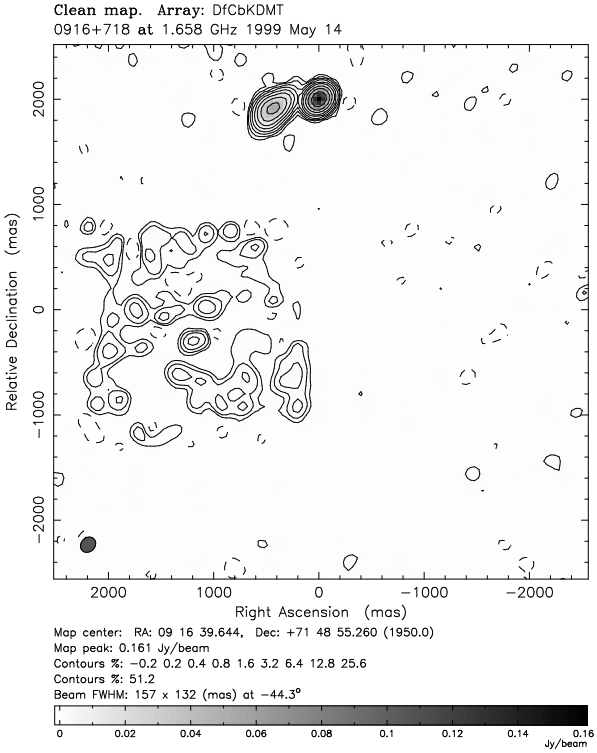
Clean map. Array: DfCbKDMT
0916+718 at 1.658 GHz 1999 May 14
Relative Declination (mas)
Right Ascension (mas)
Map center: RA: 09 16 39.644, Dec: +71 48 55.260 (1950.0)
Map peak: 0.161 Jy/beam
Contours %: −0.2 0.2 0.4 0.8 1.6 3.2 6.4 12.8 25.6
Contours %: 51.2
Beam FWHM: 157 x 132 (mas) at −44.3°
Jy/beam

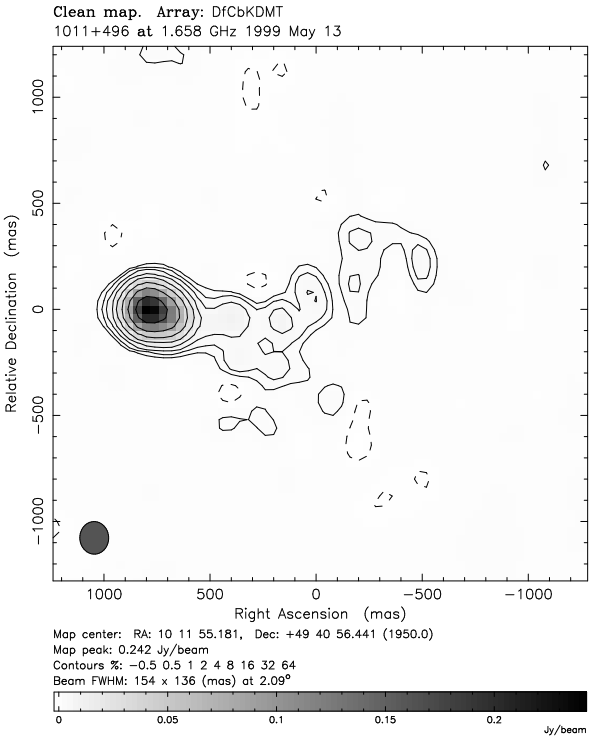
Clean map. Array: DfCbKDMT
1011+496 at 1.658 GHz 1999 May 13
Relative Declination (mas)
Right Ascension (mas)
Map center: RA: 10 11 55.181, Dec: +49 40 56.441 (1950.0)
Map peak: 0.242 Jy/beam
Contours %: −0.5 0.5 1 2 4 8 16 32 64
Beam FWHM: 154 x 136 (mas) at 2.09°
Jy/beam

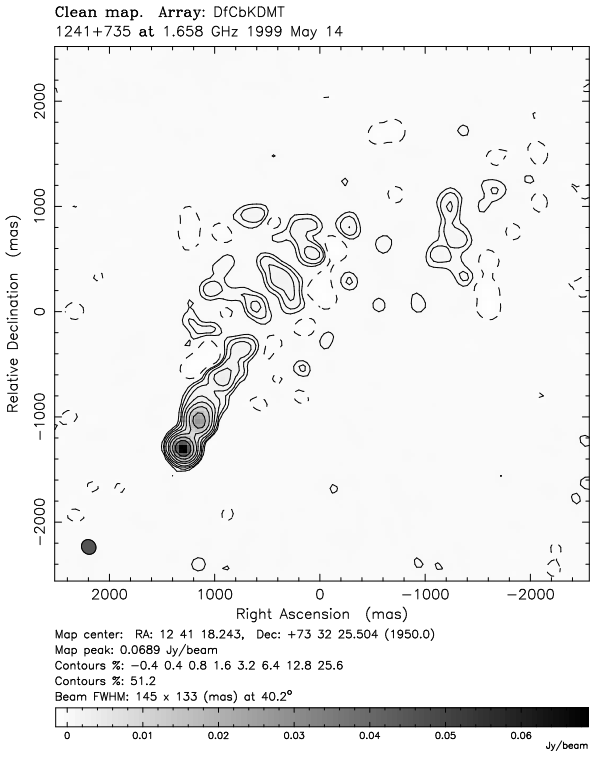
Clean map. Array: DfCbKDMT
1241+735 at 1.658 GHz 1999 May 14
Relative Declination (mas)
Right Ascension (mas)
Map center: RA: 12 41 18.243, Dec: +73 32 25.504 (1950.0)
Map peak: 0.0689 Jy/beam
Contours %: −0.4 0.4 0.8 1.6 3.2 6.4 12.8 25.6
Contours %: 51.2
Beam FWHM: 145 x 133 (mas) at 40.2°
Jy/beam

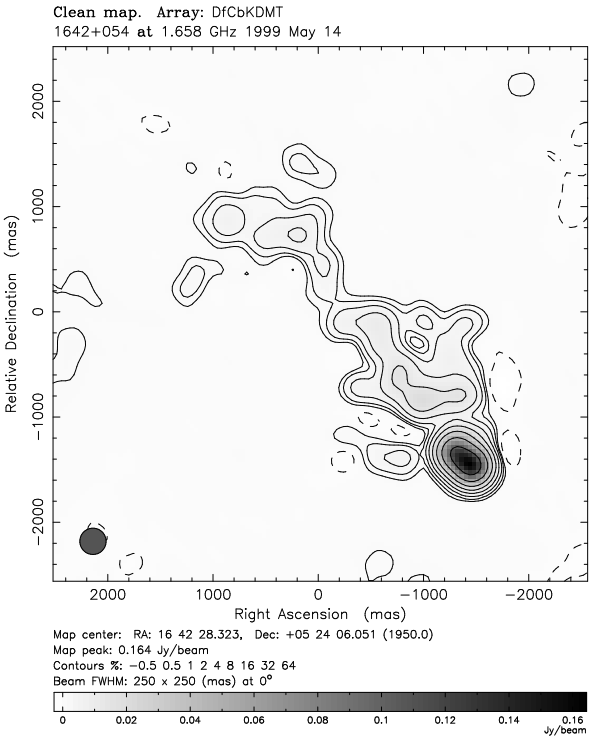
Clean map. Array: DfCbKDMT
1642+054 at 1.658 GHz 1999 May 14
Relative Declination (mas)
Right Ascension (mas)
Map center: RA: 16 42 28.323, Dec: +05 24 06.051 (1950.0)
Map peak: 0.164 Jy/beam
Contours %: −0.5 0.5 1 2 4 8 16 32 64
Beam FWHM: 250 x 250 (mas) at 0°
Jy/beam

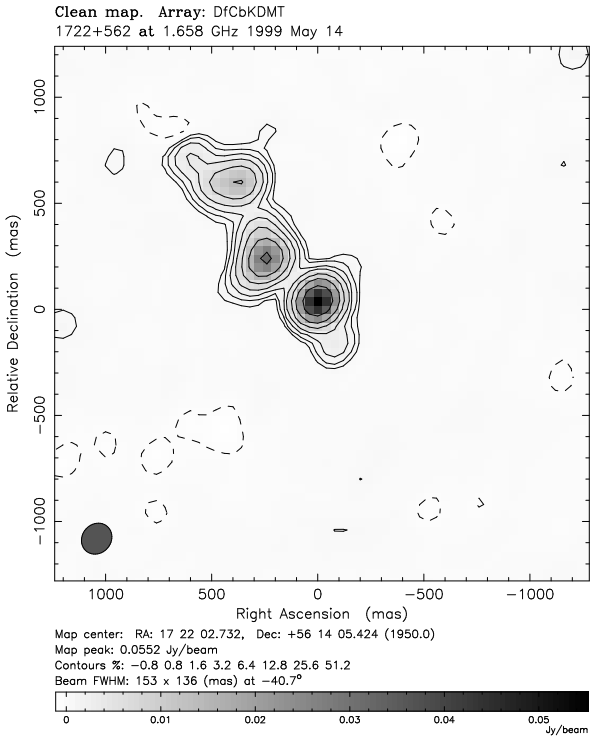
Clean map. Array: DfCbKDMT
1722+562 at 1.658 GHz 1999 May 14
Relative Declination (mas)
Right Ascension (mas)
Map center: RA: 17 22 02.732, Dec: +56 14 05.424 (1950.0)
Map peak: 0.0552 Jy/beam
Contours %: −0.8 0.8 1.6 3.2 6.4 12.8 25.6 51.2
Beam FWHM: 153 x 136 (mas) at −40.7°
Jy/beam

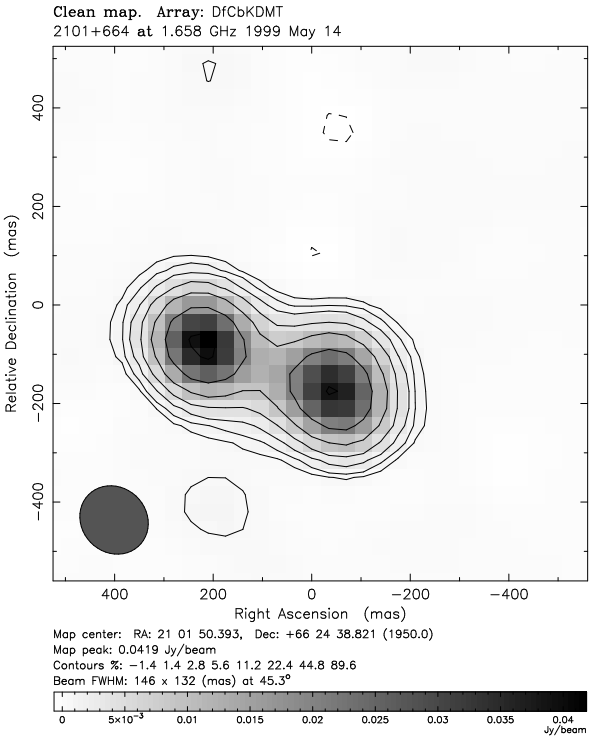
Clean map. Array: DfCbKDMT
2101+664 at 1.658 GHz 1999 May 14
Relative Declination (mas)
Right Ascension (mas)
Map center: RA: 21 01 50.393, Dec: +66 24 38.821 (1950.0)
Map peak: 0.0419 Jy/beam
Contours %: −1.4 1.4 2.8 5.6 11.2 22.4 44.8 89.6
Beam FWHM: 146 x 132 (mas) at 45.3°
Jy/beam

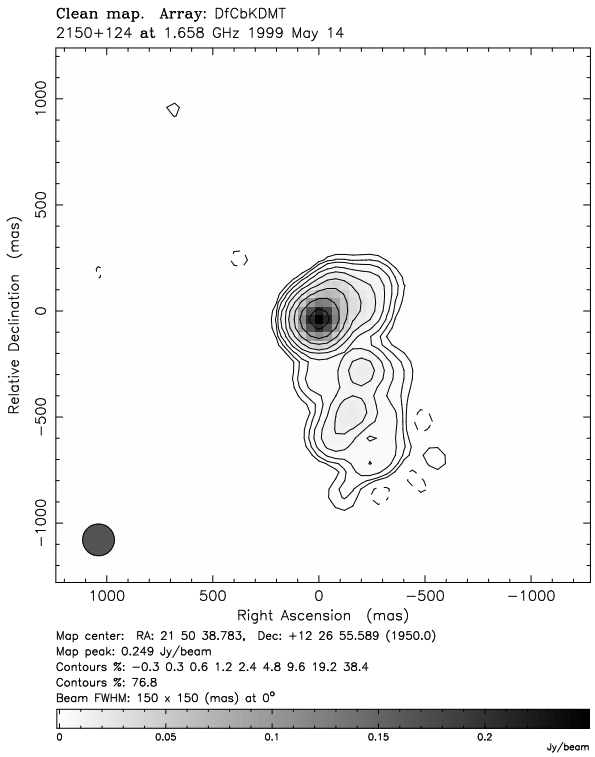

Figure 2.4: The new MERLIN L-band maps of 13 of the largest sources in the 55-source sample. Some of the maps have been convolved with circular beams for clarity.

Table 2.5: The sources in the 55-source sample that have data in FIRST. Unresolved sources are marked with '—' in the 'structure' column while resolved sources get a short description and have images presented in Figure 2.5.

Source	S_{peak} (mJy/beam)	S_{total} (mJy)	Structure
B0732+237	893.37 ± 0.141	916.38	—
B0819+082	289.99 ± 0.141	296.80	—
B0821+394	1403.96 ± 0.442	1456.09	—
B0824+355	913.49 ± 0.234	938.43	two blobs; sep. 10"
B0831+557	7998.29 ± 0.778	8254.60	—
B0905+420	153.81 ± 0.180	222.62	elongated
B1003+174	567.29 ± 0.151	584.17	—
B1010+287	571.61 ± 0.198	621.82	—
B1011+496	385.85 ± 0.154	398.16	—
B1058+245	457.21 ± 0.151	468.48	—
B1143+446	309.35 ± 0.141	327.31	Complex. WAT?
B1150+095	755.25 ± 0.306	800.41	—
B1211+334	1372.84 ± 0.298	1417.99	—
B1212+177	1011.02 ± 0.182	1027.30	—
B1233+539	421.22 ± 0.141	432.55	—
B1317+199	736.59 ± 0.153	759.83	—
B1342+341	262.85 ± 0.151	267.73	—
B1504+105	403.75 ± 0.143	408.39	—
B1628+216	467.64 ± 0.134	482.86	—
B1638+124	2090.83 ± 0.519	2159.33	—
B1722+562	149.35 ± 0.143	176.38	two blobs; sep. 10"

2.1.6 FIRST (on-going survey)

Some of the 55-source sample objects have been observed within the FIRST survey (e.g. (Becker et al. 1995)), made with the VLA at 21 cm, roughly with 5" resolution. In Table 2.5 and Figure 2.5 we present all data existent, relevant to our sample, as of December 2000. We note that the sky coverage of FIRST is roughly on RA = 7h–18h; Dec = 0°–60°.

2.2 Abell 2390

Since the project was submitted not much more was done on this source. The paper is well under preparation. B2151+174 is the radio counterpart of the cD galaxy in the rich cluster Abell 2390, which has a strong X-ray cooling flow. The size of the radio component, $\sim 1.6\ h_{75}^{-1}$ kpc, and the fact that it has symmetric structure around a bright core (Augusto et al. 1999) made us classify this source as a small MSO. However, remapping the source with MERLIN 1.6 GHz data alone (from the MERLIN+EVN 1.6 GHz taken in 30th May 1997) lead us to a different conclusion: there seems to be a clear 'blob' about $\sim 9.5\ h_{75}^{-1}$ kpc (3 arcsec) away, NE

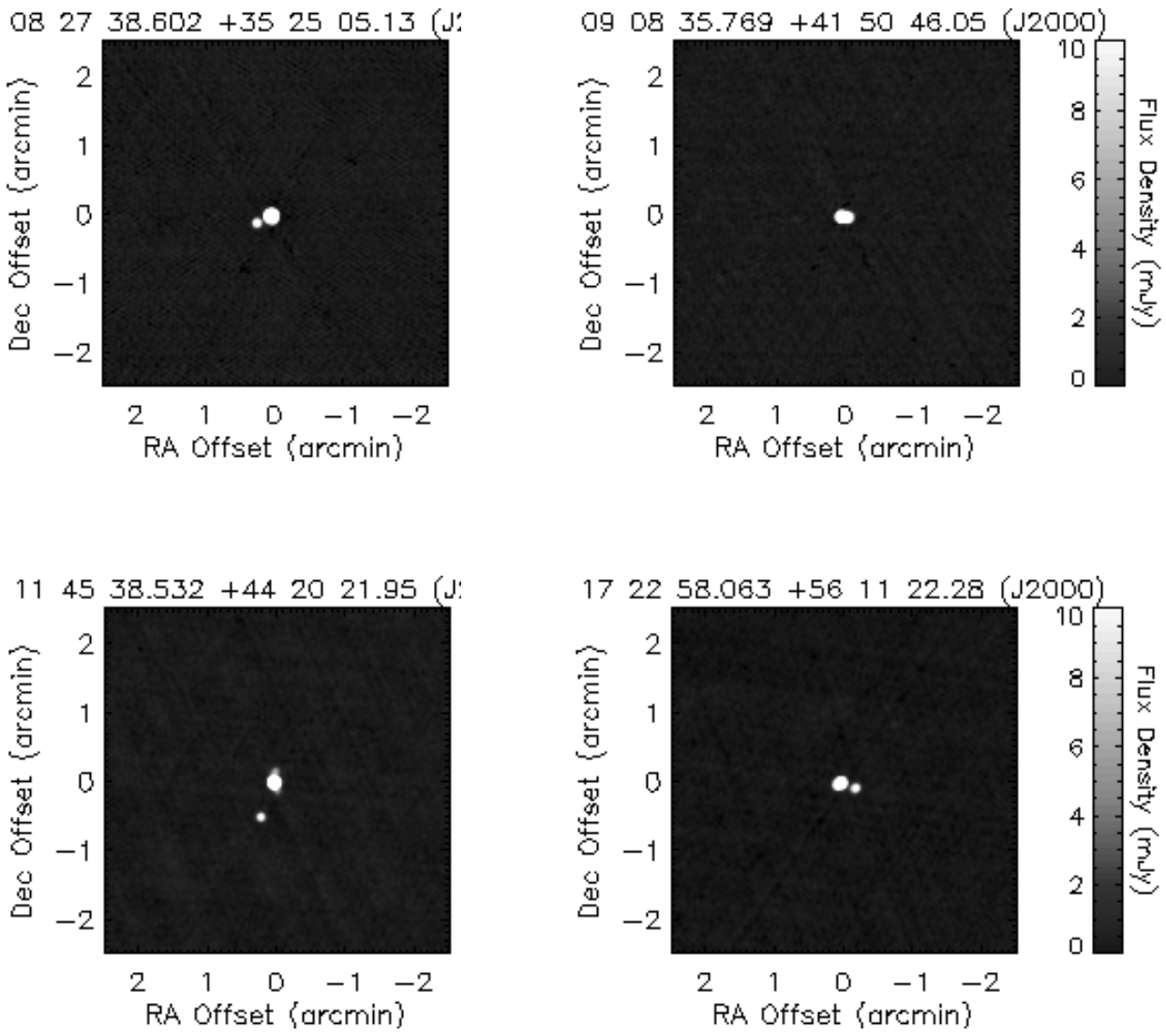

Figure 2.5: The FIRST 21 cm VLA images of the sources in our sample which showed resolved structure (see Table 2.5).

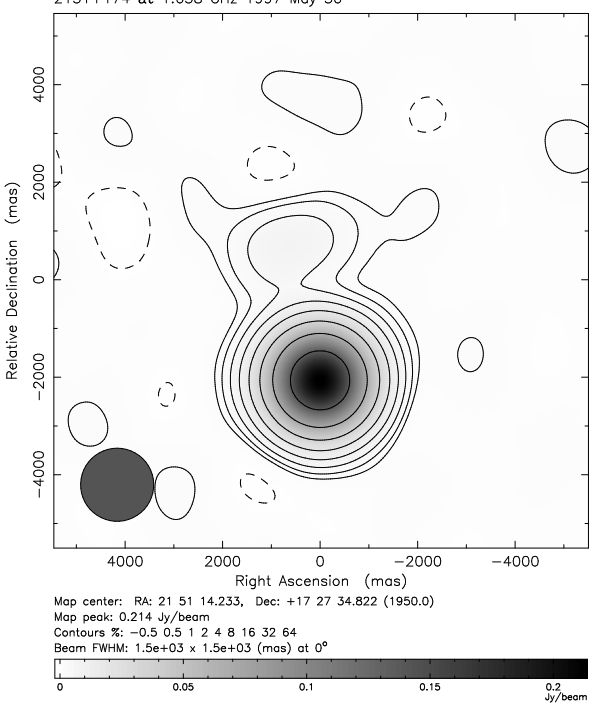

Figure 2.6: The MERLIN L-band map of B2151+174 when convolving the natural MERLIN beam with a circular one about 10 times larger to see the 'blob' more clearly. The compact 'core' in this map contains all previously mapped radio components of B2151+174. The p.a. of the 'blob' with respect to the core is +14°.

of the radio core at p.a. +14° — Figure 2.6. Given the small size of the source, it still could be an MSO, but now quite a few times larger than what we first thought.

This new discovery prompted a literature search for any optical counterpart coincident or close to the radio jet (be it an optical jet or an interacting galaxy), since Abell 2390 has been extensively mapped in the optical, including with the HST. The first step was to search for counterparts on the optical data from several telescopes presented in (Le Borgne et al. 1991), namely their Table 3 and Figure 5: no galaxy exists in the quadrant 5 arcsec east and 10 arcsec north of the cD (c.f. Figure 2.6). Nevertheless, Figure 5 of (Le Borgne et al. 1991) shows some 'noisy' components fairly well aligned with the radio jet, at p.a. $\sim$ +15–25° and about $\sim$20–30 h_{75}^{-1} kpc away from the core (Figure 2.7). The fact that there were several components aligned seemed to make it something real, since the likelihood of noise components aligning in such a way is very small. In fact, existing HST images revealed this 'noise' as real: a lensed straight arc of a background galaxy — Figure 2.8.

It is rather surprising that within 7 arcmin ($\sim$ 1 Mpc) of the cD Abell 2390, although there are about 850 optical galaxies, only five radio sources are found with the NVSS at 1.4 GHz ($>$ 1 mJy). One of these is, obviously, B2151+174 — the strongest by far. The remaining four sources are quite far from the cD ($> 73.5''$ or $> 230\ h_{75}^{-1}$ kpc) and quite weak ($S_{1.4} < 15$ mJy). Only one of these is probably identified with a galaxy (nr. 564 of (Le Borgne et al. 1991), which is only $\sim 4''$ away from the radio position; there is a $\sim 2''$ error in the optical positions of the paper). The small number of radio sources seen in the field of Abell 2390 is surprising,

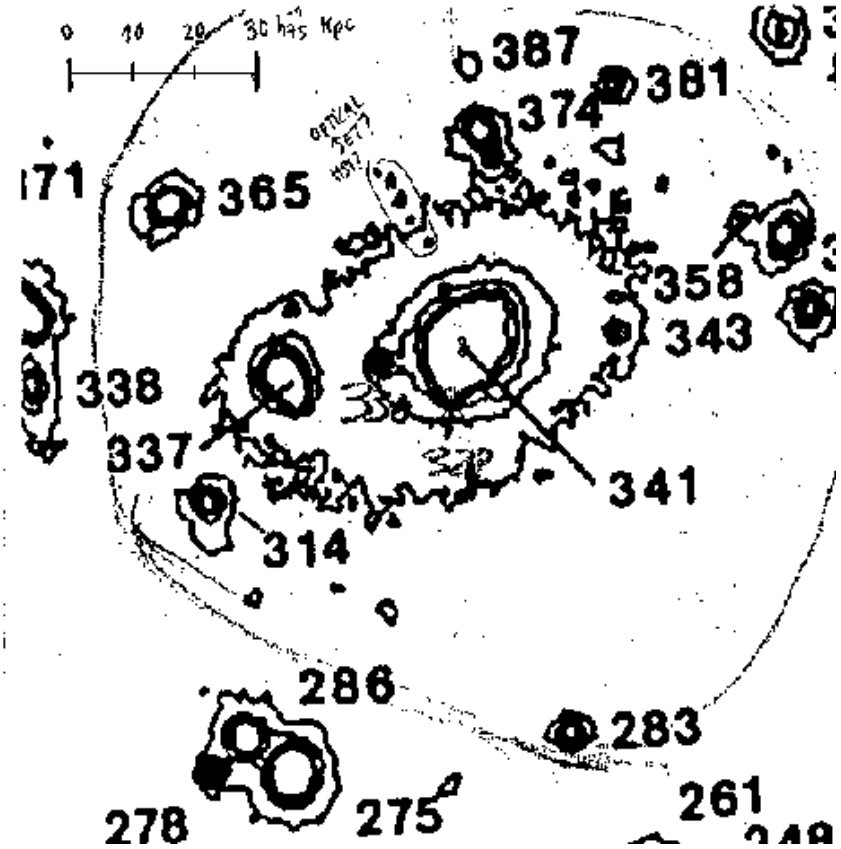

Figure 2.7: A magnified version of Figure 5 in (Le Borgne et al. 1991). The linear scale was produced after converting the angular scale shown in their paper. Notice how well aligned are the 'noisy' components at p.a. $\sim +15$–20° with respect to the centre of the cD galaxy where the radio core also lies. North is to the top.

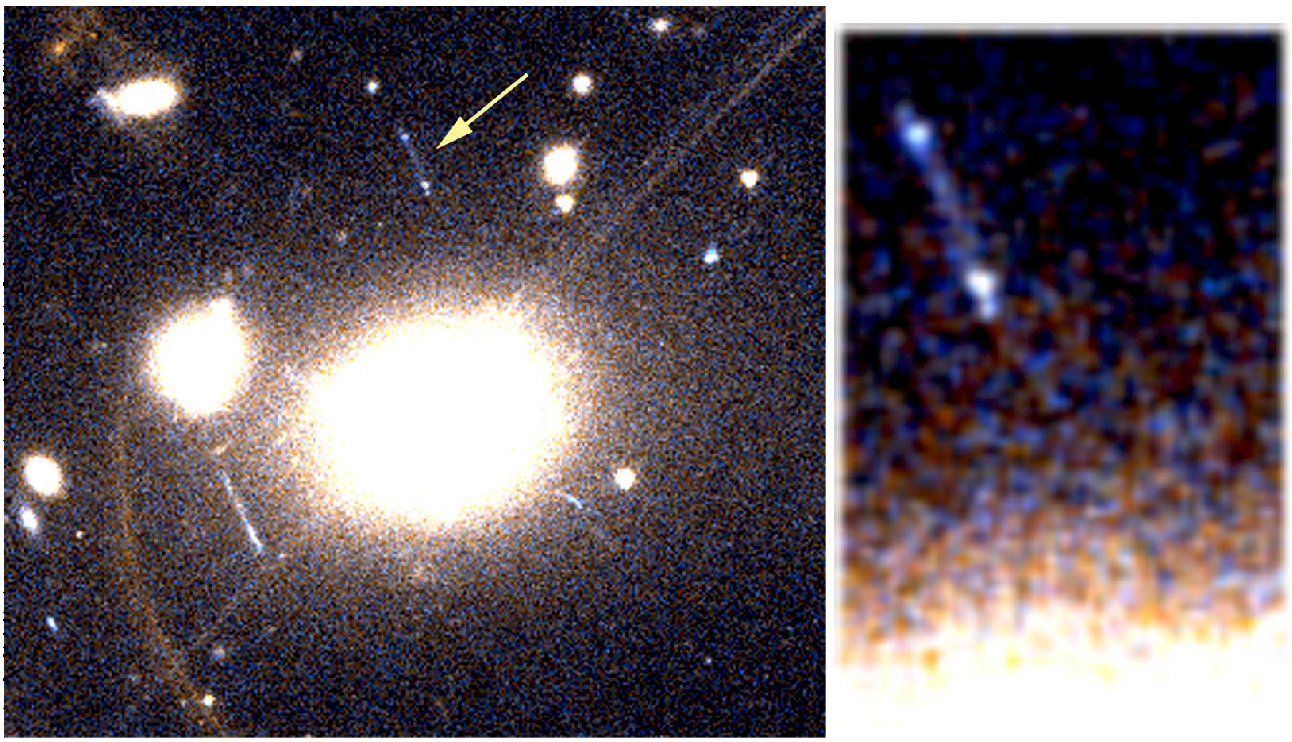

Figure 2.8: The central galaxies of Abell 2390 with the HST (V and I filters combined — true colour; (Smail 2000)). The cD is the dominant galaxy. North is *not* to the top on this image (c.f. Figure 2.7). The arc (marked with an arrow on the left) is shown in more detail on the right image, after some mild image processing (blur; contrast+27; contrast+27; blur). The arc is on the exact place of the 'noisy' blobs in Figure 2.7.

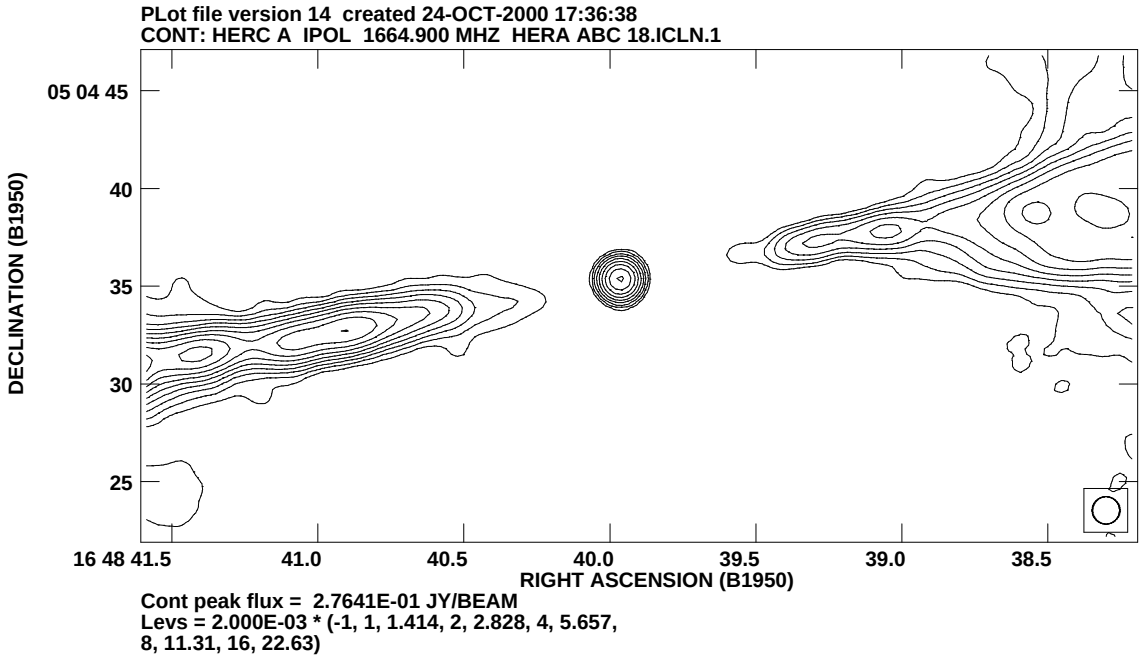

Figure 2.9: The VLA 18 cm map of Hercules A, combining data taken with A, B and C configurations. The resolution is 1.4". Note that the core is unresolved.

given such a large and massive cluster, dominated by strong and weak lensing effects, namely through magnification. Only its low redshift ($z \sim 0.2$) might be against lots of efficient lensing since the cross section for lensing may not be large enough to significantly magnify distant and very distant radio objects behind it.

2.3 Hercules A (to be abandoned in 2001)

This was part of the work of Dr. Nektaria Gizani inside our project. Since she has left the project in Sep 2000, it is not possible to consider Her A for the future. What was done in 2000: although we had hopes that Hercules A was not a guaranteed time proposal for Chandra, this did not happen. Hence, the observations will be conducted, reduced and (likely) published by elseone. In order to model Her A jets and magnetic fields, we need to probe as close to the centre of activity as possible (pc-scale environment). Previous VLA data hinted that the core might actually be compact (Figure 2.9). MERLIN+EVN 1.6 GHz observations have been conducted and the data reduced. Indeed, Her A shows a compact VLBI core and short jets, which are misaligned with the VLA jets. These results will be published soon.

Table 2.6: Journal of observations with the Nordic Optical Telescope (NOT) of B2231+359 (BVRI photometry). Dates: 13-15 Sep 1999. The exposure times are in seconds.

Source	B	V	R	I
B2231+359	600	600	600	900

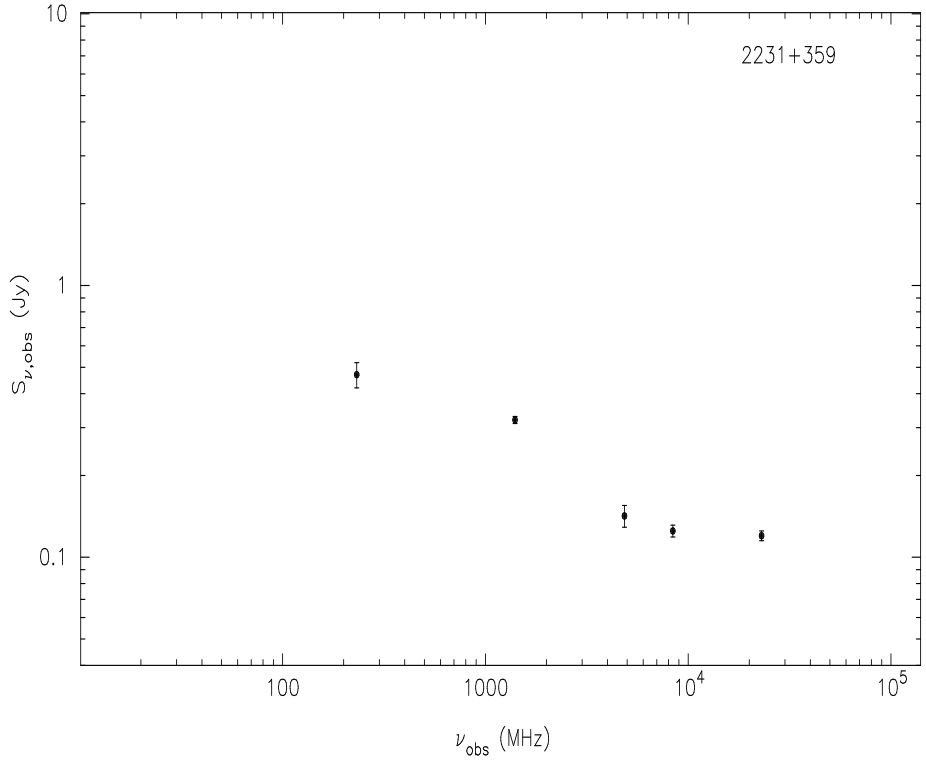

Figure 2.10: The spectra of B2231+359 — see Table 2.2 for references. The 232 MHz data point (Zhang et al. 1997) is actually a lower limit, since it corresponds to a peak flux density.

2.4 M87 high-z replica (B2231+359)

This source is not, strictly, inside the 55-source sample because of the spectral index criterion (it has $\alpha_{1.4}^{4.85} = 0.65 > 0.5$ — 'new' value only). Nevertheless, as presented in (Augusto et al. 1999), its properties are encouraging enough for a detailed study. This source is actually included in the general kpc-scale sample of 154 radio sources from JVAS/CLASS (flat + steep spectra) — Appendix B. In Table 2.6 we present the optical results for B2231+359. The (updated) spectra of B2231+359 is presented in Figure 2.10. B2231+359 is an optical empty field on the Palomar Observatory Sky Survey (POSS) and hence we are planning to determine its spectra with the William Hershel Telescope (WHT) to start with (see Chapter 3).

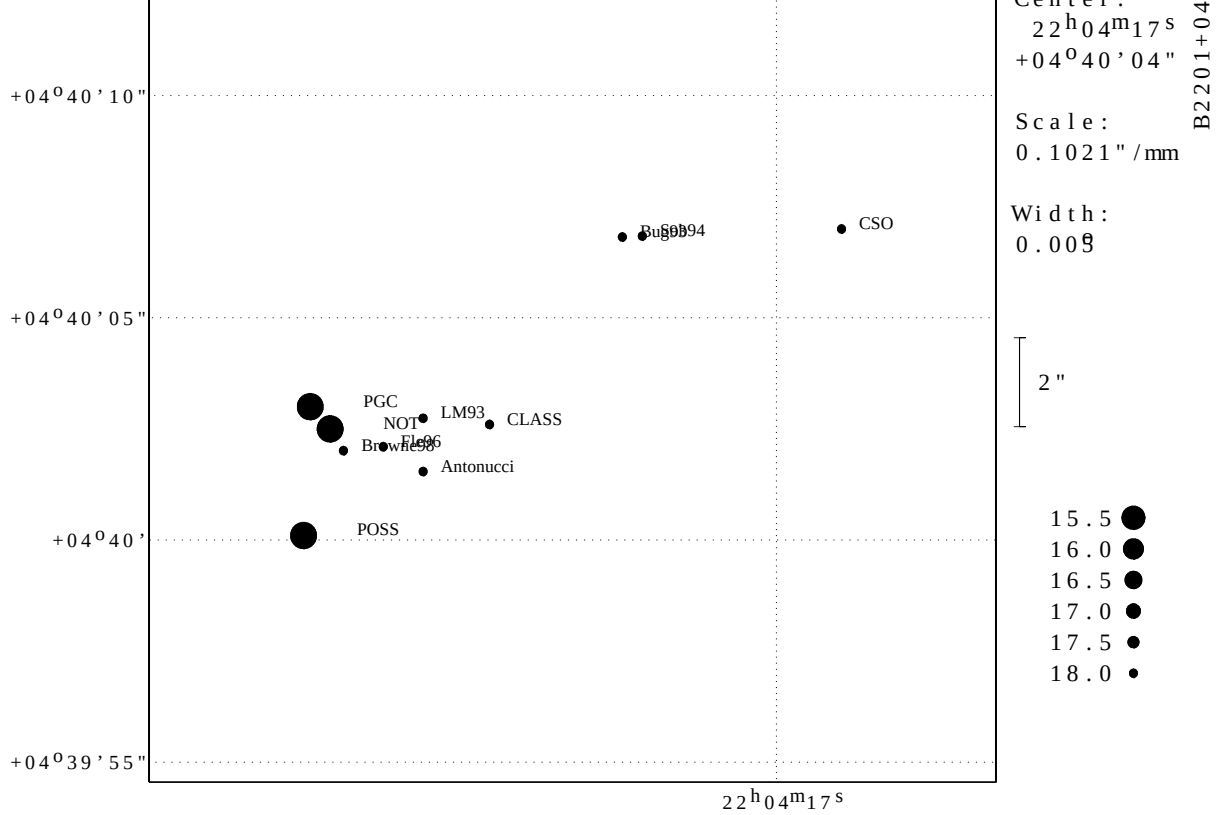

Figure 2.11: The different positions quoted in the literature for B2201+044. Labels are all on the right side of the relevant point whose size reveals the uncertainty. Optical: NOT (our astrometry from 4 bands), POSS (measured by us in the DSS file) and PGC (Paturel et al. 1999). Radio: CLASS (catalogue: Browne, pers. comm.), CSO (Augusto et al. 1998), Antonucci (Antonnucci 1985), Fle96 (Fletcher et al. 1996), LM93 (Laurent-Muehleisen et al. 1993), Bug93 (Bugaenko et al. 1993), Sob94 (Soboleva et al. 1994) and Browne98 (Browne et al. 1998).

2.5 B2201+044 (new interest)

This 55-source sample source has been classified as a BLLac object in the extensive literature about it. We were puzzled by the huge difference in the (Augusto et al. 1998) position and our NOT astrometry on the observations of this object. In fact, it was so much that we were not sure of what its optical identification really was. Likely a bright galaxy (Section 3.1) but certainly we should check all radio/optical positions available to solve the puzzle. In Figure 2.11 we present all positions and conclude that, likely, (Augusto et al. 1998) position is not correct and we should rather use the 'CLASS group' positions. The explanation for all disagreement is, no doubt, related to the fact that this source is highly variable and very large (with structure extending to arcmin).

B2201+044 is one example of a source in our sample with valuable HST WFPC2 observations, which have revealed an optical jet, coincident with the radio jet (Scarpa et al. 1999).

Chapter 3

The optical side

3.1 Photometry

We got two proposals accepted to do BVRI photometry with the Nordic Optical Telescope (NOT) of as many of the 55 sources as possible. We had two runs, three nights in 13-15 Sep 1999 and two nights in 1-2 Feb 2000. On the first run, one of the nights was only half successful due to some clouds and technical problems with the Hirac system. Otherwise, the run was quite successful, with fair seeing (at $\sim$ 1"). Although in the second run we were able to observe virtually all the time, the seeing was poorer (at $\sim$ 2"). Of the 55 sources, 42 were observed ($\sim$ 76%) — see Table 3.1 — and only 13 objects are then left, which we list in Table 3.2. Furthermore, in Table 3.3, we also list the 5 parent sample objects that were observed — we have taken these objects from a control JVAS/CLASS subsample of 100 objects, most of which already have redshift and/or photometric information (see Appendix G for the full list of the 100 objects that represent the parent sample, as well as their optical properties, if known).

The data reduction is now complete. Standard bias and flat-field corrections were done. The I images suffer from fringing which was correted for most of the frames. In order to identify the optical counterpart of the radio sources, astrometric solutions were found for all the frames. This was performed using a semiautomatic process inside IRAF developed by Eduardo González-Solares & Ismael Pérez-Fournon (IAC), which looks at the USNO catalogue. The position errors are typically 0.3–0.4". Once the sources were identified, aperture photometric measurements were performed.

The conclusions from the two observation runs as regards photometry are: i) the second run was not photometric due to dust in the atmosphere; ii) the limiting magnitudes are around 23 mag in R and I — not all objects were seen in B or V. Tables 3.4 and 3.5 list broad-band magnitudes for the observed objects after correction by Galactic extinction. For the empty fields, limiting magnitudes at the 5σ level are given.

Some examples of the images obtained are shown in Figure 3.1. There are 6 bright extended objects, which are all elliptical galaxies (B0352+825, B1011+496, B1241+735, B1744+260, B2201+044, B2247+140). Other 13 objects are compact and brighter than $V \sim 17-18$ and they may be either QSOs or compact galaxies (B0351+390, B0819+082, B0824+355, B0905+420, B1003+174, B1143+446, B1801+036, B1812+412, B1857+630, B1928+681, B2101+664, B2150+124, B2210+085). The remaining 23 sources are either faint ($V > 20$) or empty fields, except

Table 3.1: Journal of observations with NOT of the 55-source sample. Dates: 13-15 Sep 1999 and 1-2 Feb 2000 (italic). We have observed 42 sources with BVRI photometry. The exposure times are in seconds.

Source	B	V	R	I
B0112+518			600	900
B0127+145	300	300	300	300
B0205+722	600, 900	300, 600	300	300
B0218+357	600	300	300	300
B0225+187	600, 1800	300, 600	600	300
B0233+434			600	900, 900
B0345+085			900	900
B0351+390	600	600	600	600
B0352+825	200	200	200	300
B0418+148			900	900
B0429+174	600	600	600	900
B0529+013	600	300	300, 600	500
B0638+357			900	900
B0732+237	*600, 900*	*600*	*900, 900*	*900, 900*
B0817+710	*600, 900*	*600, 600*	*900, 900*	*900, 900*
B0819+082	*600*	*600*	*600*	*600*
B0824+355	*900*	*600*	*600*	*600*
B0905+420	*600*	*600*	*600*	*600*
B1003+174	*600*	*600*	*900*	*900*
B1010+287	*900, 600, 261*	*600, 600*	*900, 900*	*900, 900, 900*
B1011+496	*200*	*200*	*200*	*300*
B1058+245			*900*	*900, 900*
B1143+446	*300*	*300*	*300*	*900*
B1241+735	*200*	*200*	*200*	*200*
B1317+199	*600*	*900*	*900, 900*	*900, 900*
B1628+216	300	300	300, 300, 300	10, 300, 300
B1642+054			600	900
B1722+562	300	300	300	300
B1744+260	300	300	300, 300	300
B1801+036	300	300	300	300
B1812+412	300	300	300	300
B1857+630	500	300	300	300
B1928+681	600	600	600	520.2
B1947+677			600, 600, 900	
B2101+664	300	300	300	300
B2112+312	600	600	600	600
B2150+124	600	600, 600	600	600
B2201+044	200	200	200	200
B2205+389	900	900	900	900
B2210+085	300	300	300	300
B2247+140	300, 300		300	300
B2345+133	500	300	300	300

Table 3.2: The 13 objects of the 55-source sample that still lack BVRI photometry data, together with their POSS identifications (G — galaxy; R-BSO — red-blue stellar object; EF — empty field), visual magnitudes and relevant extra optical information extant in the literature.

Source	POSS id.	V (mag)	General information
B0046+316	G	15.0	BVRI; well studied Sy2; z=0.015
B0116+319	G	16.0	VJHK; elliptical; z=0.0592
B0821+394	BSO	18.0	K; z=1.216
B0831+557	G	17.5	JHK; z=0.242
B0916+718	BSO	18.5	z=0.594
B1150+095	BSO	18.0	UBV; QSO; z=0.698
B1211+334	BSO	17.2	UBVRI+HST; QSO; z=1.598
B1212+177	RSO	20.0	
B1233+539	BSO	19.0	
B1342+341	BSO	19.5	
B1504+105	odd	16.0	
B1638+124	EF	(21.8)	rHK; compact gal; z=1.152
B2151+174	G	17.5	VI+I.R.+HST; cD Abell 2390; z=0.231

Table 3.3: Journal of observations with NOT of the parent sample. Dates: 1-2 Feb 2000. We have observed 5 sources with BVRI photometry. The exposure times are in seconds.

Source	B	V	R	I
B0327+364			900	900
B0353+289	600	600	600	600
B0442+071	900, 900	600	900	900
J0554+689	600	600	600	600
B0635+351	600	600	900	900

Table 3.4: Photometry of 42 sources in the 55-source sample.

Name (B1950.0)	B	$\sigma(B)$	V	$\sigma(V)$	R	$\sigma(R)$	I	$\sigma(I)$	comments
0112+518	-	-	-	-	>21.9	-	>21.5	-	
0127+145	19.89	0.013	19.75	0.022	19.36	0.013	18.79	0.022	
0205+722	19.94	0.114	19.45	0.049	19.43	0.059	19.07	0.059	
0218+357	21.40	0.068	20.32	0.056	19.62	0.047	18.47	0.048	
0225+187	23.12	0.080	21.67	0.061	20.47	0.031	19.29	0.031	
0233+434	-	-	-	-	22.6	0.200	21.69	0.110	
0345+085	-	-	-	-	22.7	0.200	20.82	0.070	
0351+390	18.35	0.022	18.53	0.044	18.66	0.136	18.50	0.017	
0352+825	16.64	0.014	15.46	0.044	14.818	0.136	11.66	0.017	
0418+148	-	-	-	-	>22.6	-	>21.7	-	
0429+174	21.25	0.097	20.60	0.072	20.01	0.059	19.18	0.053	
0529+013	22.0	0.207	21.8	0.302	21.49	0.146	21.5	0.303	
0638+357	-	-	-	-	21.6	0.137	20.9	0.147	
0732+237	24.4	0.202	>23.1	-	20.94	0.044	19.93	0.061	
0817+710	23.73	0.104	21.55	0.063	20.69	0.038	19.41	0.050	
0819+082	21.10	0.042	19.55	0.040	18.78	0.038	18.11	0.027	
0824+355	20.90	0.035	19.90	0.044	20.06	0.042	19.35	0.032	
0905+420	18.931	0.029	18.414	0.039	18.305	0.037	17.86	0.027	
1003+174	20.69	0.035	19.93	0.044	19.571	0.039	18.686	0.027	
1010+287	22.41	0.166	22.18	0.136	21.65	0.077	20.38	0.076	
	22.27	0.058	-	-	-	-	20.26	0.056	
1011+496	16.305	0.029	15.983	0.039	15.570	0.037	15.051	0.025	
1058+245	-	-	-	-	22.33	0.126	20.88	0.056	
1143+446	18.780	0.030	18.006	0.039	17.510	0.037	16.805	0.025	
1241+735	16.453	0.030	15.610	0.039	14.876	0.037	14.023	0.025	
1317+199	22.24	0.100	21.92	0.155	20.39	0.038	19.42	0.055	
1628+216	-	-	-	-	-	-	-	-	bright star in the field
1642+054	-	-	-	-	22.821	0.136	22.25	0.130	
1722+562	20.82	0.058	20.24	0.044	20.144	0.045	19.63	0.048	
1744+260	18.93	0.056	16.81	0.044	16.22	0.044	15.94	0.045	
1801+036	17.71	0.056	17.17	0.044	16.84	0.043	16.56	0.045	
1812+412	20.28	0.058	20.34	0.063	19.60	0.047	19.33	0.059	
1857+630	19.46	0.014	18.912	0.045	18.65	0.136	18.36	0.024	
1928+681	20.74	0.032	19.37	0.044	18.59	0.136	17.70	0.017	
1947+677	-	-	-	-	>23.6	-	-	-	
2101+664	16.83	0.013	16.64	0.013	16.49	0.013	16.37	0.013	
2112+312	22.89	0.300	23.10	0.400	21.79	0.140	21.89	0.350	
2150+124	19.88	0.014	19.83	0.044	19.91	0.136	19.41	0.024	
2201+044	>22.7	-	>22.2	-	>22.2	-	>21.0	-	at the radio position (Augusto et al. 1998)
2205+389	-	-	-	-	-	-	22.00	0.111	
2210+085	19.277	0.013	18.485	0.011	17.851	0.010	17.051	0.009	
2247+140	16.996	0.055	-	-	16.367	0.043	15.861	0.044	
2345+113	22.04	0.060	20.54	0.041	19.604	0.019	18.535	0.021	

Table 3.5: Photometry of parent sample sources (including B2231+359).

Name	B	$\sigma(B)$	V	$\sigma(V)$	R	$\sigma(R)$	I	$\sigma(I)$	comments
0327+364	-	-	-	-	23.2	0.262	>21.8	-	
0353+289	19.66	0.031	18.99	0.040	18.72	0.038	18.53	0.027	
0442+071	20.46	0.048	20.16	0.049	19.75	0.038	19.20	0.055	
	20.48	0.035	-	-	-	-	-	-	
J0554+689	20.23	0.035	20.00	0.044	19.49	0.038	19.19	0.032	
0635+351	20.87	0.058	19.93	0.056	19.47	0.044	18.69	0.047	
2231+359	23.22	0.260	23.02	0.300	22.75	0.240	>22.1	-	

B1628+216 which will require a lot of work to classify it because of the presence of a very bright star in the field.

Figure 3.2 shows colour-colour diagrams for the sample objects. Objects have well defined $V-R$ and $R-I$ colours in the range 0-1, but have a wide range of values of the $B-V$ colour index. There are two red objects, with $B-V \sim 2.2$ (B1744+260 and B0817+710). As we only have 5 observed parent sample objects, it is premature to extract any conclusion about the CSO/MSO colour information.

We plan to do near-IR photometry of all sources (preferably) since the preliminary results indicate that the vast majority are quite faint up to the I band. To get good photometric redshift estimates we need at least to go up to the K-band. We will submit proposals to the Telescopio Nazionale Galileo (TNG) and possibly also to the Calar Alto Telescopes, using either (or both) the 3.5m OMEGA or the 2.2m MAGIC. We should be able to successfully observe the sample in two nights. UKIRT (in Hawaii) would be a possibility despite the fact that it cannot observe above 60° declination. This is not much of a problem for our $0° < dec < 90°$ sample, since only nine out of the 55 objects have $dec > 60°$. To complete the BVRI photometry (13 objects left — Table 3.2) we can use the IAC 80 cm or the JKT 1 m telescopes.

3.2 Spectroscopy

As regards spectroscopy, among the 35 sources in the 55-source sample without any spectral information are sixteen POSS empty fields (almost half). Furthermore, eleven other have POSS visual magnitudes around 20 mag. Only eight of the 35 sources have $V \leq 19$. During 2000 we submitted two spectroscopic proposals to La Palma telescopes that were rejected. Given this, we plan to submit a spectroscopic proposal to the 4.2 m WHT at La Palma, using ISIS for all our 27 faint sources (EF + 20 mag). If possible, we would also like to get the spectra of the eight brightest sources, since this would be very fast with the WHT. Otherwise, we can apply later for time to do spectroscopy for these latter using the NOT (Alfosc) or the Isaac Newton Telescope (INT) using IDS. We also have left as an option, for the faintest sources, the 3.5m Calar Alto Telescope, using TWIN.

In Table 3.6 we show all literature knowledge on 20 of the 55 objects of the sample about their spectra (all but one have secure redshifts). Their actual optical spectra are reproduced from

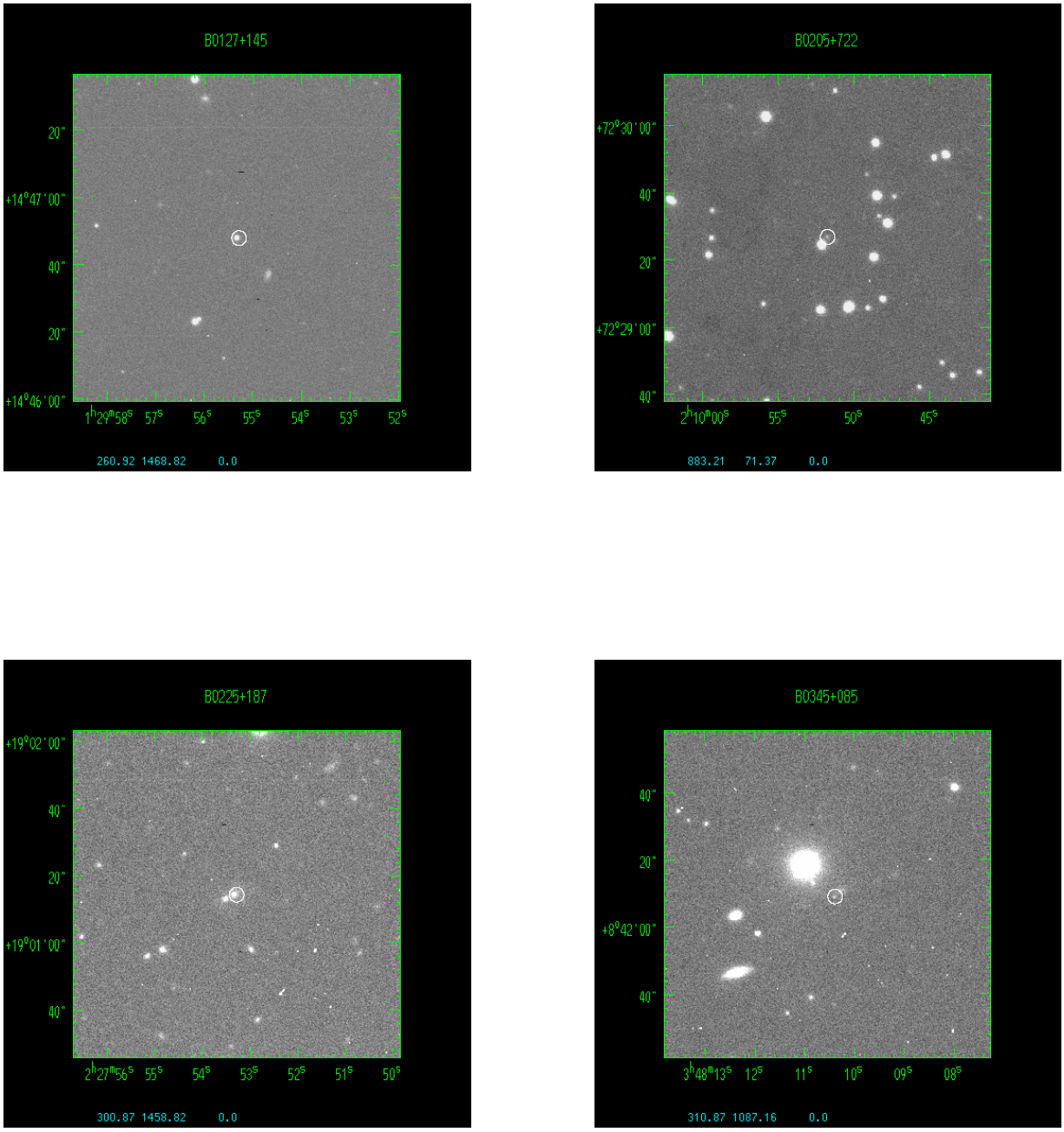

Figure 3.1: Examples of the images obtained with NOT. From upper left to bottom right the bands were: R, I, R and R.

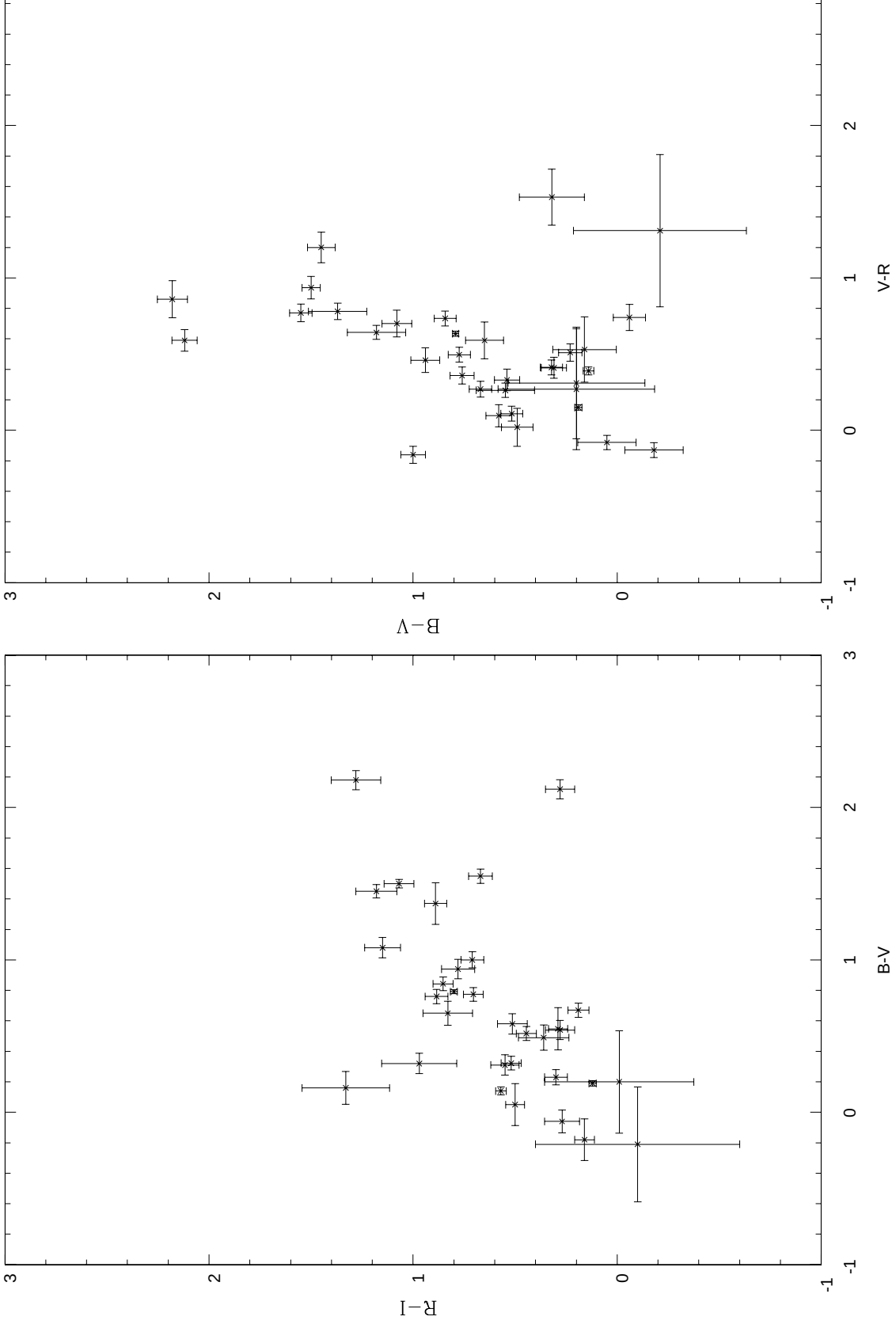

Figure 3.2: Colour-colour plots for the 42 objects of the 55-source sample that were observed with NOT.

the literature in Figure 3.3.

3.3 HST

To study the prospects for observing the 55 objects with the Hubble Space Telescope (HST), we will first use a list of positions of all 1665 parent sample objects from JVAS/CLASS1 to see if any of these has been observed with the HST before (by cross-correlating the positions with the HST archive). There are several cases that have been observed for sure: over 7 cases of gravitational lenses in JVAS/CLASS1 that are also in the parent sample, and a few other well known objects in our sample. It may well be that we decide that the only relevant science that we expect, a priori, to get from the HST with this 55-source sample might come from narrow-band observations of only a few sources at a suitable redshift — we might then expect to detect optical/radio alignements in our sources due to star-formation prompted by the radio jets from the interaction with the ISM (e.g. (Capetti et al. 1996)). An argument against using CSO/MSOs to get this science might be their ages (likely all younger than 10^6 yr). Nevertheless, there should be no such problem with the NLR probes which constitute more than half of our 55-source sample.

Table 3.6: Spectroscopy of 20 sources of the 55-source sample available in the literature. See Figure 3.3 with their spectra plots. References (on their optical spectra information): 1 — (de Bruyn & Sargent 1978); 2— (Koski 1978); 3— (Tran 1985); 4— (Cid Fernandes et al. 1998); 5— (Gelderman & Whittle 1994); 6— (Vermeulen et al. 1996); 7— (Browne et al. 1993); 8— (Lawrence 1996); 9— (Wills & Wills 1976); 10— (Allington-Smith et al. 1998); 11— (Whyborn et al. 1985); 12— (Falco et al. 1998) & Falco, Pers. Comm.; 13— (Stickel & Kühr 1996); 14— (Machalski 1991); 15— (Hook et al. 1996); 16— (Foltz et al. 1986); 17— (Marcha et al. 1996); 18— (Stickel et al. 1996); 19— (Henstock et al. 1997); 20— (Crawford et al. 1999); 21— (Veron-Cetty & Veron 1993).

Name	Telescope	Exposure	Redshift	Class	Ref.	Radio	Comments
B0046+316	Lick 3m	32 min	0.015	Sy2	1–4	CSO	Mrk 348
B0116+319	Kitt Peak 2.1m	3000 s	0.0592	Elliptical	5	CSO	4C31.04
B0205+722	Palomar 5m	1300 s	0.895	Galaxy	6	MSO	
B0218+357	(WHT 4.2m)	(hrs)	0.936	?	7–8	CJ	lensed CJ
B0821+394	McDonald 2.7m	40 min	1.216	QSO	9	CJ	
B0824+355	INT 2.5m	?	2.249	QSO	10	MSO	
B0831+557	Lick 3m	3 hrs	0.242	Galaxy	11	FRI	
B0905+420	MMT	?	0.7325	QSO	12	CJ	
B0916+718	Stewart 2.3m MMT	?	0.594	QSO	13	CJ	
B1011+496	WHT 4.2m AAT 3.6m	?	0.2 ?	BLLac	14	CJ	bad spectra
B1143+446	WHT 4.2m	300–600 s	0.30	QSO	15	CJ	
B1150+095	McDonald 2.7m	40 min	0.698	QSO	9	CJ	
B1211+334	McDonald 2.7m	40 min	1.598	QSO	9, 16	CJ	
B1241+735	MMT	600–1200 s	0.075	Galaxy	17	CJ	
B1638+124	Kitt Peak 4m	?	1.152	Galaxy	18	CJ	
B1744+260	MMT	600–1200 s	0.147	Galaxy	17	CJ	
B1812+412	INT 2.5m	2000 s	1.564	QSO	19	CJ	
B2151+174	INT 2.5m	1000 s	0.231	Galaxy	20	MSO	cD of Abell 2390
B2201+044	ESO 3.6m	30 min	0.028	BLLac/Sy1	21	CJ	
B2247+140	Kitt Peak 2.1m	2400 s	0.237	QSO	5	CJ	4C14.82

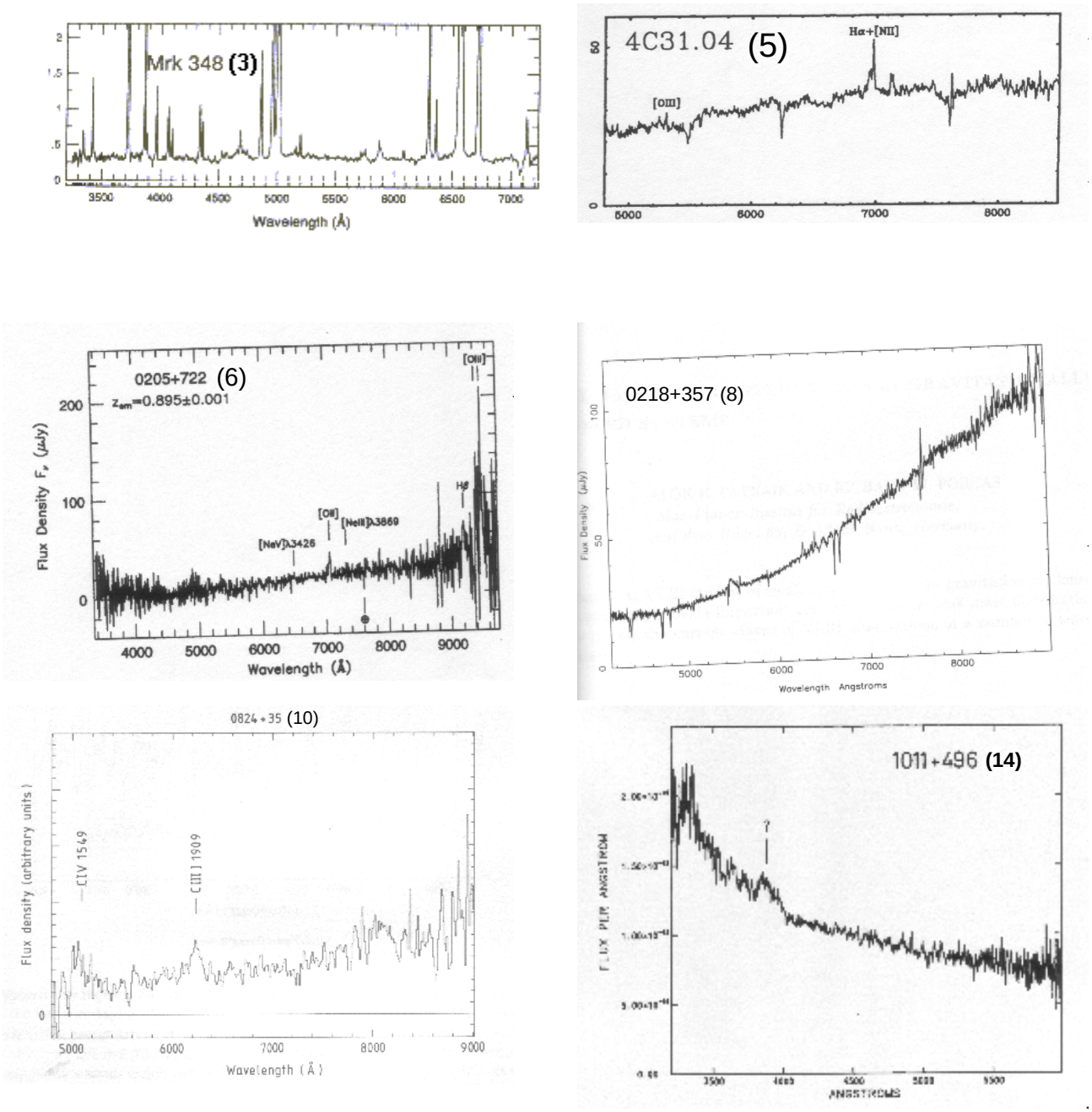

Figure 3.3: The spectra existent in the literature for the 20 sources in the 55-source sample, as listed in Table 3.6. The spectra shown have the reference as in Table 3.6 — source (ref), except for B0905+420 (12). Some sources are known by other names as shown in Table 3.6. Three of the sources have no spectra available but rather some lines mentioned in the literature which allowed their redshift determination. These sources, not shown here, are the following: B0821+394 (9), B0916+718 (13) and B1150+095 (9).

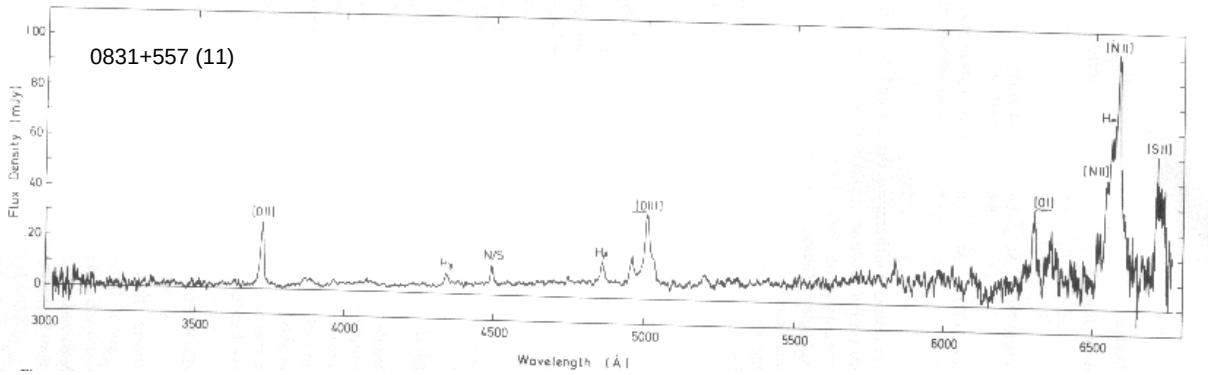
0831+557 (11)
Flux Density (mJy)
Wavelength (Å)
[OII]
[OIII]
[OIII]
[OII]
[NII]
[NII]
[SII]

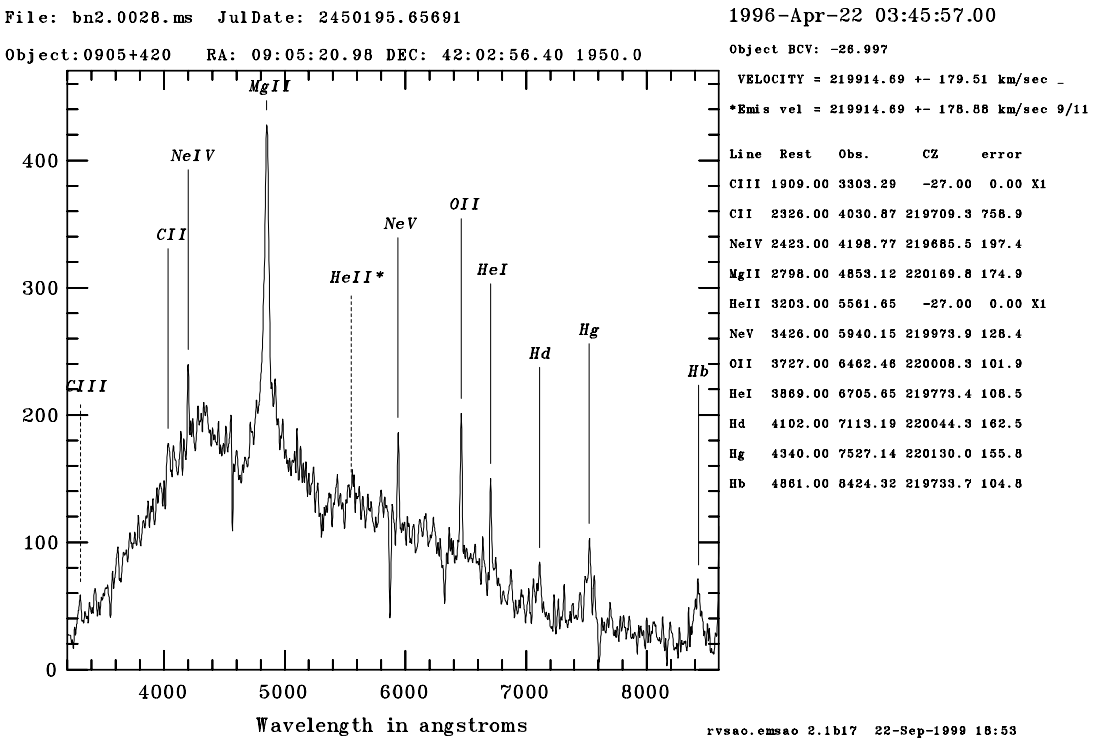
File: bn2.0028.ms JulDate: 2450195.65691
1996-Apr-22 03:45:57.00
Object:0905+420 RA: 09:05:20.98 DEC: 42:02:56.40 1950.0
Object BCV: -26.997
VELOCITY = 219914.69 +- 179.51 km/sec
*Emis vel = 219914.69 +- 178.88 km/sec 9/11
Line Rest Obs. CZ error
CIII 1909.00 3303.29 -27.00 0.00 X1
CII 2326.00 4030.87 219709.3 758.9
NeIV 2423.00 4198.77 219685.5 197.4
MgII 2798.00 4853.12 220169.8 174.9
HeII 3203.00 5561.65 -27.00 0.00 X1
NeV 3426.00 5940.15 219973.9 128.4
OII 3727.00 6462.46 220008.3 101.9
HeI 3869.00 6705.65 219773.4 108.5
Hd 4102.00 7113.19 220044.3 162.5
Hg 4340.00 7527.14 220130.0 155.8
Hb 4861.00 8424.32 219733.7 104.8
MgII
NeIV
CII
CIII
HeII*
NeV
OII
HeI
Hd
Hg
Hb
Wavelength in angstroms
rvsao.emsao 2.1b17 22-Sep-1999 18:53

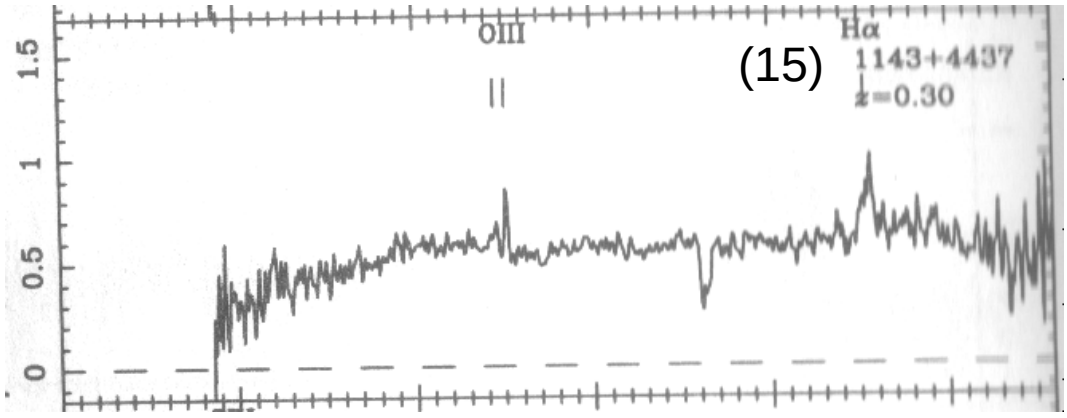
OIII
(15)
Hα
1143+4437
z=0.30

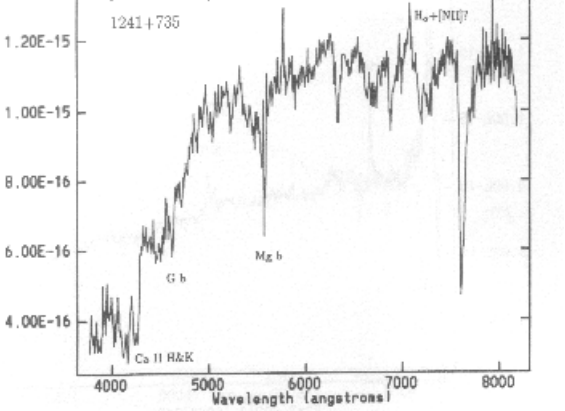
1241+735
1.20E-15
1.00E-15
8.00E-16
6.00E-16
4.00E-16
Hδ+[NII]?
Mg b
G b
Ca II H&K
4000
5000
6000
7000
8000
Wavelength (angstroms)

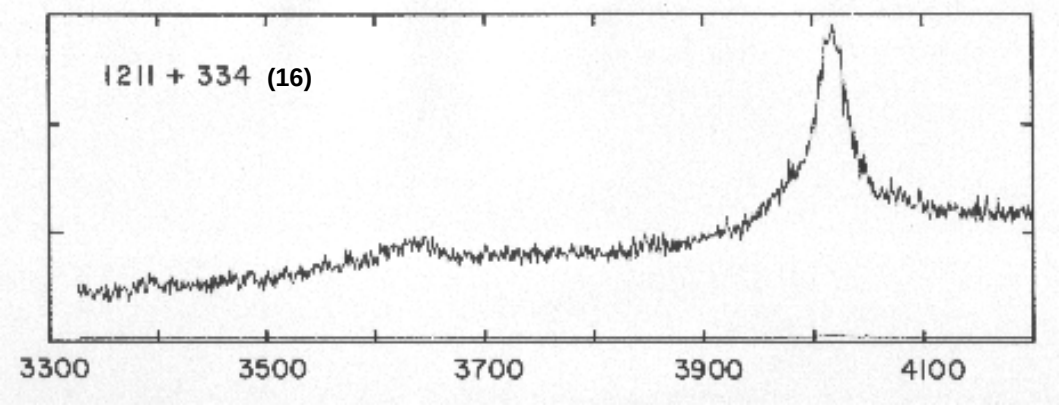
1211 + 334 (16)
3300
3500
3700
3900
4100

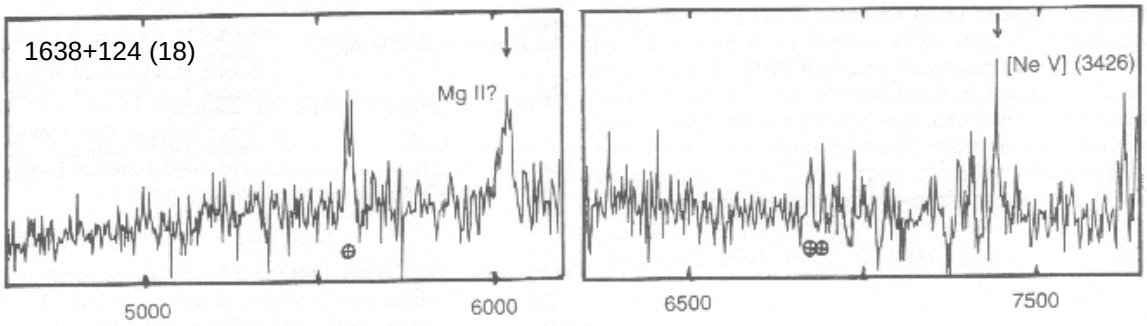
1638+124 (18)
Mg II?
[Ne V] (3426)
5000
6000
6500
7500

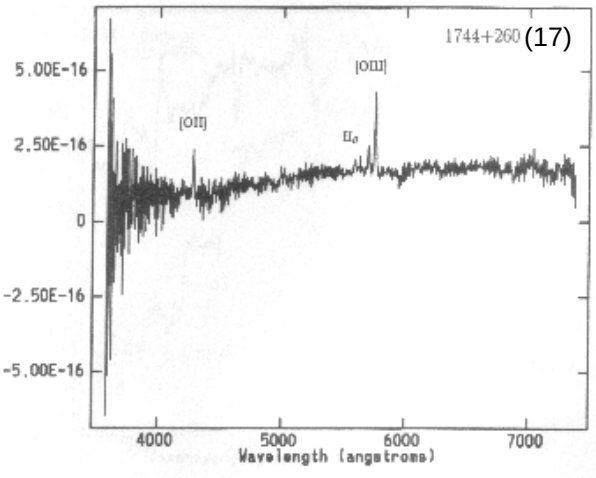
1744+260 (17)
5.00E-16
2.50E-16
0
-2.50E-16
-5.00E-16
[OII]
[OIII]
Hδ
4000
5000
6000
7000
Wavelength (angstroms)

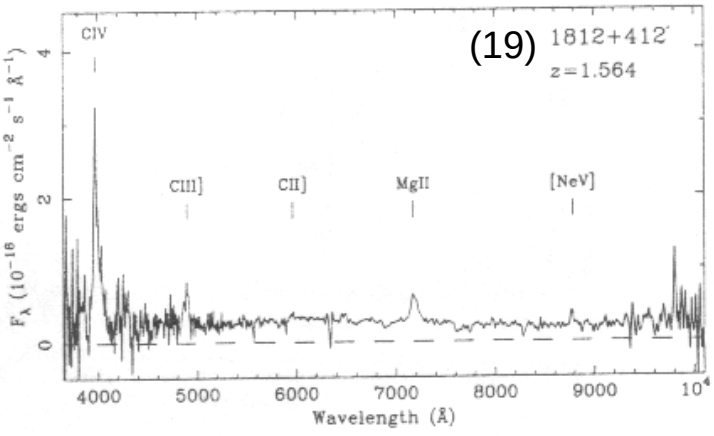
(19) 1812+412
z=1.564
CIV
CIII]
CII]
MgII
[NeV]
F_λ (10^{-16} ergs cm^{-2} s^{-1} Å^{-1})
0
2
4
4000
5000
6000
7000
8000
9000
10^4
Wavelength (Å)

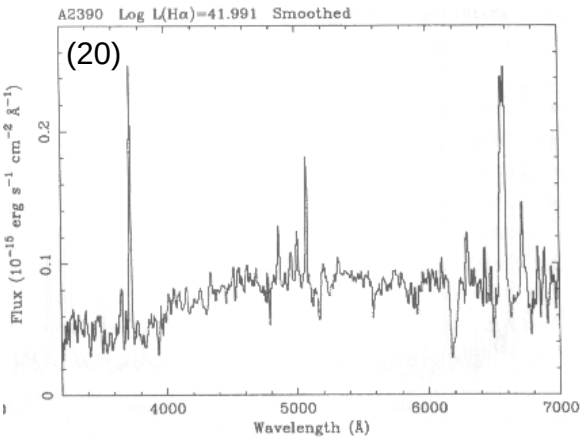
A2390 Log L(Hα)=41.991 Smoothed
(20)
Flux (10^{-15} erg s^{-1} cm^{-2} Å^{-1})
0
0.1
0.2
4000
5000
6000
7000
Wavelength (Å)

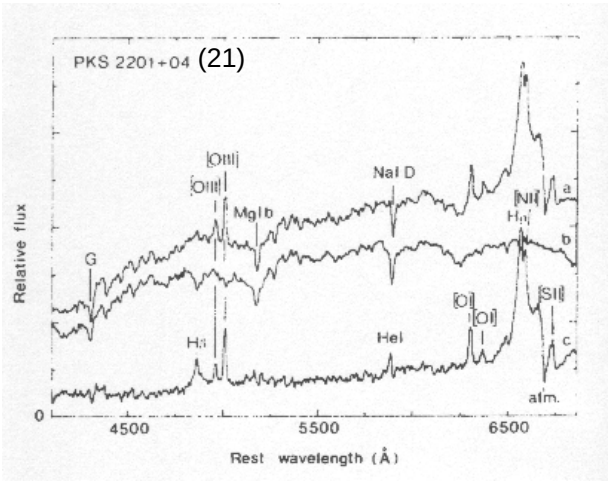
PKS 2201+04 (21)
[OIII]
[OIII]
Mg I b
Na I D
[NII]
Hη
a
b
G
[OI]
[OI]
[SII]
c
Hδ
He I
atm.
Relative flux
0
4500
5500
6500
Rest wavelength (Å)

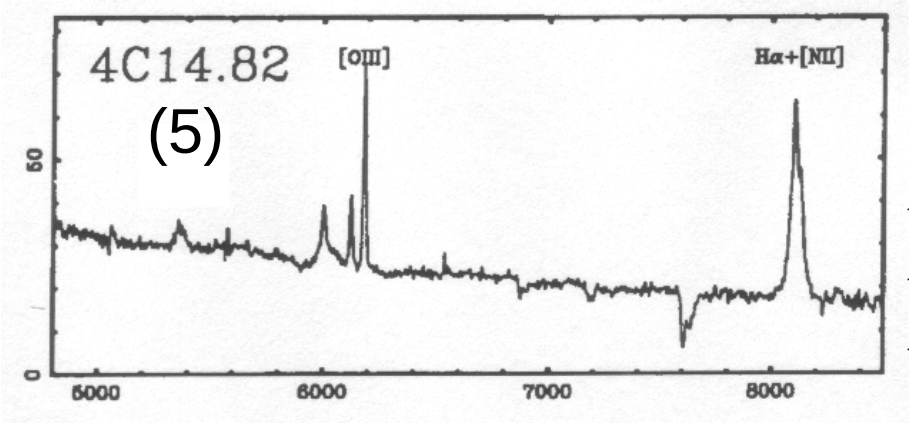
4C14.82
(5)
[OIII]
Hα+[NII]
50
0
5000
6000
7000
8000

Chapter 4

The X-ray side

We overviewed the current and past status of X-ray missions: in the past, the main mission by far, ROSAT, produced two main surveys: i) an all-sky survey (RASS) with sensitivity of $\sim 10^{-12}$ erg/cm^2/s; ii) a Pointed Observations survey covering $\sim 10\%$ of the sky with sensitivity $\sim 10^{-14}$ erg/cm^2/s. Unfortunately almost all sample sources have lower X-ray fluxes than the limit of RASS. We should search for them in the Pointed catalogue, just in case we were lucky. A strong detection in RASS was B2151+174 (Abell 2390). Future/undergoing surveys will use new missions all with similar sensitivities at $\sim 10^{-15}$ erg/cm^2/s: i) Chandra/AXAF ($\sim 1\%$ of the sky); ii) Newton/XMM ($\sim 5\%$ of the sky). Hence, unless we are lucky (we will still have to wait for a while — e.g. Newton will only give results around 2002), we do not expect any sky survey to detect our sources. We must identify and classify the best targets in our sample for X-ray observations (optically and with radio) by showing them to be somehow unusual before applying for X-ray time. Since most sources are bound to have structures on ~ 1" scales, Chandra is the ideal instrument to apply for, especially because we must have a case where we actually expect to see structure and not just a point X-ray source. Nevertheless, for some specific cases, we may get away with a spectroscopic only proposal, since spectroscopy comes by default with all imaging in X-rays. Only in the very distant future might we have all-sky surveys more sensitive than ROSAT: i) ABRIXAS-2 (sensitivity $\sim 10^{-13}$ erg/cm^2/s); ii) PANORAM-X (sensitivity $\sim 10^{-14}$ erg/cm^2/s); and perhaps other new missions.

As regards possibilities of X-ray detection for our sources with, for example, Chandra, the fact that most sources likely have a luminosity peak at radio wavelengths does not imply that the same will happen at X-rays. Our sources likely are just 'ordinary' (faint) in what regards to X-ray emission. The fact that many are quite young (the CSO/MSOs) fights against the possibility of detection of X-ray emission from them.

In general radio sources, there is a huge scatter in L_{radio}/L_X (greater than 10^4). This is especially true for QSO/radio-galaxies not dominated by beaming effects. When these effects dominate, like in BL Lacs, then we can estimate the expected X-ray flux from extrapolation of the radio synchrotron spectra.

The interests of X-ray information for our objects are several: i) together with the spectral index information for our sources, compare radio-quiet and radio-loud objects, namely CSO/MSOs, and check for evolution; ii) N_H (hydrogen column density) will give us information of the circumnuclear material; we might study the area where the jets come from and learn about the inclination angle of the source; iii) study the (cluster) environment by finding extended structure

corresponding to gas around the host galaxy of our object; this might give us information about the intracluster medium, and in some cases about the intergalactic medium as well.

As a summary of the ideal case for a proposal in X-rays for our sample: i) an arcsecond-sized radio galaxy; this will likely excluded almost all CSO candidates and leave MSOs for study; well-justified spectroscopy could be conducted for the CSOs; ii) the source should be embedded in a cluster, so that we can predict the luminosity expected from the richness and redshift alone; this should be easy to verify in the optical imaging data, picking out the cases where there is a galaxy excess around the object; iii) for some specific objects, a good case might be made.

We plan to submit a proposal to Chandra for the most interesting sources in the sample. We must have the literature search on CSSs, etc. completed as well as the crucial optical information (namely spectra) at hand. We may also consider submitting a proposal for XMM, mainly for getting spectra of the most promising CSO/MSOs, but these observations (like the ones with Chandra) will only be conducted in 2002 (or later), formally after the end of the project.

Chapter 5

General Discussion

There was a lengthy discussion on the variability and 'α-problem' issues. In particular, looking back at Table 2.3 it is particularly striking the case of B1628+216, for example, which has an 'old-α' of 0.16 and a 'new' one of 0.63 (see Appendix A). We should really look into detail to each one of the fifteen cases in Table 2.3 on trying to explain these huge jumps. Several explanations were put forward and need checking: i) the error bars in the old and the new references might explain at least some 'jumps' — we must check them all and use error bars for each of the 'old' and 'new' α and see if they are, or not, still inconsistent; ii) the difference in beam sizes of the flux density measurement surveys might be a reason: for example, (White & Becker 1992) used a beam 3–4 times larger than NVSS did; confusing sources might have been included in the former survey, hence explaining the jumps from the steep to the flat side (as in Figure 2.3). Finally, still related to this variability issue, it seems clear than a new type of radio object exists: 'sub-kpc' steep sources (like the objects in Figure 2.3 and Appendix B). Perhaps the Compact Steep Spectrum source class of object should be extended from the traditional 1–15 kpc in size down to pc-scales. At least, if we use the strict $\alpha < 0.5$ definition for CSOs.

We have also discussed the X-ray observing prospects for our sample and concluded that we must do some a priori literature search among the few papers published about X-ray observations of related objects like CSSs and such, and (few) CSO/MSOs themselves. We can hope to get some flux predictions (most crucial) from this knowledge.

Sub-mm searches for the core of the 55 sources was put forward as an alternative to current multiwavelength radio projects. For example, the experience with one of our sources (B2151+174) with SCUBA has detected emission that is mostly attributed to dust (not much service for the core finding idea) since it is a bright radio source ($\sim$200 mJy). If there is no dust, probably the detection is not possible and the core finding hypothesis does not work. If most objects in the sample lie at $z \sim 0.5$–1.0, as it seems to be the case, then it is not likely that they will have a lot of dust to be detected. However, the highest redshift objects in the sample may be well worth a follow up.

We could conceivably do the same search we have conducted on the parent sample for other samples like the Lockman Hole or the Galactic North Pole samples. For example, although our sample is bound to 'complete' the statistics of CSOs at all scales, MSOs will still be a rare 'beast' (at least the largest ones). A good hypothesis would be to find such objects in those samples since the data exist.

Another interesting point is that our study of CSO/MSOs (with others currently being undertaken) will reveal the density of CSOs in the Universe at given epochs, most crucial for their evolution story. Maybe we can already get an estimate for VLBI CSOs for existing data. Unfortunately CSO/MSOs seem to be rare and, for example, we do not expect to find any in the small existing fields of deep X-ray surveys.

As an overall sum up of source characteristics and X-ray/other prospects (mostly based on the (Augusto et al. 1998) classification of bright/faint core CSO/MSOs and CJs): i) sources close to the plane of the sky are likely *unbeamed* (probably the faint core CSO/MSOs) and they will be excellent for the geometrical determination of the NLR sizes as described in (Augusto et al. 1999); ii) *beamed* sources, likely all CJs and bright core CSO/MSOs, will not be so good/easy to work for the NLR size determination but they will be the best candidates for X-ray observations or, at least, for estimating their fluxes (extrapolating from their sychrotron radio spectra) and put a good case forward.

Chapter 6

Conclusions and Future Work

For the near future (definitely inside the project period): i) several proposals in optical spectroscopy and imaging (BVRI+I.R.); ii) VLBA 1.6/5 GHz dual frequency proposal; iii) single dish 30-100 MHz proposals for all candidates for finding out where the turnover of their spectra lies (for the vast majority this is not known); iv) VLA and MERLIN 22 GHz for a core finding effort throughout the whole 55-source sample; v) reduce the extant OHP 1.9 m spectroscopic data on a few of the candidates and parent sample sources; vi) in preparation of a future HST proposal, browse the HST archive for all sources related to our work: the 55 sources (some have HST data) and the 1665 sources of the parent sample (many are bound to have HST data). We will start by using their known positions to write a program to go automatically through the HST archive; vii) study the possibility of good science from sub-mm observations of the 55-source sample, since they are all flat-spectrum sources — core finding may actually be rewarding at these frequencies (also looking for obscuring dust); towards this aim, we must first go through an archive like XXSCAN at IPAC, entering the list of positions for the whole samples (both the main 55-source sample and the parent sample, for control) — since it is all done automatically there is not much of an extra effort we then get the limits on the amount of dust from IRAS 60μm data (and perhaps finding dust for a number of sources!).

Other marginal things to be done in the near future: i) carry on with what we study in Appendix B: determine the 'new' parent sample and compare with 'all spectra' kpc-sources; ii) substantially improve Table D.1 by getting observation dates and placing all candidates in it, including the ones which do not show variability and the ones with no data available in NED; we must use fraccional variabilities; compactness vs. variability: when the table is completely revised, we can split the 55-source sample into two: compactness follow up studies (non-variable sources) and variability studies (variable sources); iii) produce a Table like Table E.1 for the existing MERLIN+EVN 1.6 GHz data/sources; iv) re-check WENSS data for all sources; v) 'jump' in α: use errors in $\alpha_{1.4}^{4.85}$ (new/old) before redoing the study; vi) literature search for X-ray prospects from the 55-source sample; vii) on Appendix B try to fit standard statistical distributions to the α distributions; viii) looking for the 55-source sample or parent sample in X-ray: Pointed ROSAT catalogue.

For the far future (likely outside the project period): after we have all optical information (spectral and photometric) on the 55-source sample, we should: i) get HST data on quite a number of the ones that justify good science; ii) get VLA L-band observations for the one-sided source candidates (see Appendix E) — bonus off the project; iii) VLA 74 MHz observations on

the whole sample to get overall spectra for synchrotron emission model fitting to all sources; iv) we should put up an X-ray proposal by then, since we have stronger grounds for studying the sources, e.g., the cases where a cluster or group of galaxies is seen surrounding a given object of the 55-source sample; v) possibly a sub-mm proposal.

Appendix A

Spectral index values (old and new)

Table A.1: The revised $\alpha_{1.4}^{4.85}$ values for the 55-source sample from the newest surveys, not available in (Augusto et al. 1998). In the Table, 'old' stands for results in (Augusto et al. 1998) and 'new' are the recalculations done in this report. **(1):** Source name; **(2)**, **(3):** 1.4 GHz flux densities from (White & Becker 1992) and NVSS, respectively; **(4)**, **(5):** 4.85 GHz flux densities from (Gregory & Condon 1991) and GB6, respectively; **(6):** the spectral index ($\alpha_{1.4}^{4.85}$) calculated from (2) and (4); **(7):** the spectral index calculated from (3) and (5); in this column we highlight the values that are larger than 0.5 and hence put the source out of the sample.

(1) Source (B1950.0)	**(2)** $S_{1.4}^{old}$ (mJy)	**(3)** $S_{1.4}^{new}$ (mJy)	**(4)** $S_{4.85}^{old}$ (mJy)	**(5)** $S_{4.85}^{new}$ (mJy)	**(6)** $\alpha_{1.4}^{4.85}$ (old)	**(7)** $\alpha_{1.4}^{4.85}$ (new)
0046+316	270	293	254	302	0.05	- 0.02
0112+518	328	448	206	192	0.37	*0.68*
0116+319	2826	2636	1571	1609	0.47	0.40
0127+145	706	775	536	570	0.22	0.25
0205+722	842	670	560	528	0.33	0.19
0218+357	1456	1708	1498	1480	-0.02	0.12
0225+187	292	293	160	155	0.48	*0.51*
0233+434	431	510	246	243	0.45	*0.60*
0345+085	248	243	192	207	0.21	0.13
0351+389	160	198	191	208	-0.14	- 0.04
0352+825	245	245	173	173	0.28	0.28
0418+148	460	500	310	309	0.32	0.39
0429+174	429	375	270	300	0.37	0.18
0529+013	258	264	153	162	0.42	0.39
0638+357	340	372	197	212	0.44	0.45
0732+237	878	928	552	493	0.37	*0.51*
0817+710	436	603	274	274	0.37	*0.63*
0819+082	295	295	204	192	0.30	0.35
0821+394	1381	1481	1012	1031	0.25	0.29
0824+355	866	958	746	751	0.12	0.20
0831+557	7741	8284	5780	5740	0.24	0.30
0905+420	252	230	207	222	0.16	0.03
0916+718	384	491	292	295	0.22	0.41
1003+174	497	571	337	345	0.31	0.41
1010+287	612	642	331	323	0.49	*0.55*
1011+496	382	378	286	299	0.23	0.19
1058+245	416	457	231	210	0.47	*0.63*
1143+446	405	363	305	226	0.23	0.38
1150+095	737	810	500	432	0.31	*0.51*
1211+334	1196	1404	649	627	0.49	*0.65*
1212+177	836	1011	620	501	0.24	*0.57*
1233+539	392	458	215	212	0.48	*0.62*
1241+735	518	295	345	312	0.33	- 0.05
1317+199	672	730	386	325	0.45	*0.65*
1342+341	262	270	154	148	0.43	0.48
1504+105	368	404	227	221	0.39	0.49
1628+216	300	509	245	232	0.16	*0.63*

(1) Source (B1950.0)	**(2)** $S_{1.4}^{old}$ (mJy)	**(3)** $S_{1.4}^{new}$ (mJy)	**(4)** $S_{4.85}^{old}$ (mJy)	**(5)** $S_{4.85}^{new}$ (mJy)	**(6)** $\alpha_{1.4}^{4.85}$ (old)	**(7)** $\alpha_{1.4}^{4.85}$ (new)
1638+124	2066	2071	1292	1207	0.38	0.43
1642+053	659	552	393	363	0.42	0.34
1722+562	219	200	132	125	0.41	0.38
1744+260	385	349	261	263	0.31	0.23
1801+036	462	274	250	239	0.49	0.11
1812+412	644	724	534	517	0.15	0.27
1857+630	263	296	164	160	0.38	<0.50
1928+681	533	574	319	306	0.41	*0.51*
1947+677	264	—	165	—	0.38	– -
2101+664	111	101	76	77	0.30	0.22
2112+312	440	402	255	238	0.44	0.42
2150+124	422	432	264	290	0.38	0.32
2151+174	282	236	241	220	0.13	0.06
2201+044	784	467	747	653	0.04	- 0.27
2205+389	445	553	294	291	0.33	*0.52*
2210+085	226	264	208	205	0.07	0.20
2247+140	2127	1969	1177	1240	0.48	0.37
2345+113	313	341	201	228	0.36	0.32

Appendix B

The sample without spectral selection

If we turn down the spectral criterion of (Augusto et al. 1998) and select from JVAS/CLASS1 the sources with $S_{8.4}$ >100 mJy, $\left|b^{II}\right| > 10^{\circ}$ (using the 'old' $\alpha_{1.4}^{4.85}$ values as in Table A.1) and with kpc-scale structure (90 – 160 mas) — going back to (Augusto 1996) — we get a total of 99+55 = 154 sources (and obviously a proportionally larger parent sample than the 1665-source one that we had before). Their $\alpha_{1.4}^{4.85}$ distribution is presented in Figure B.1. The distribution is well-behaved (symmetric about $\alpha \sim 0.5$), showing that the kpc-scale sources are a self-consistent population of radio sources. We could not, however, fit it with the obvious gaussian distribution using the statistical mean and standard deviation for its parameters (μ=0.57; $\sigma = s_{n-1}$ =0.284, for 153 sources, since one has no data) — rejected at the 95% confidence level, using a χ^2-test. We will work on this in the future, trying to get the best possible approximation from standard statistical distributions.

We should point out that the JVAS/CLASS are flat spectrum aimed radio surveys and they bias against sources with $\alpha_{1.4}^{4.85} > 0.5$. This stands out in Figure B.1 by the fact that the centre of the distribution is not sitting at the classic $\alpha \sim 0.7$ of the general population of radio galaxies (FRII, in particular) but it is centred on $\alpha \sim 0.6$, just off the limit of the α criterion of (Augusto et al. 1998).

Nevertheless, we will determine in the future the new (extended) parent sample for the criteria of (Augusto et al. 1998) without the spectral one, and conduct similar studies as the one in this paper comparing the 154-source and the new parent samples. Most important will be the direct comparison of the α distributions of both samples to make sure that the mean of Figure B.1 is actually due to sample selection biasing from JVAS/CLASS and not to the instrinsic physics of the kpc-sized population of radio sources. In this context, it is important to note the other distribution in the same Figure: the one for α (new) since this is not gaussian or symmetrical (it is actually skewed). It has a mean of μ=0.50 and a standard deviation of s_{n-1} =0.283 (152 sources). It is actually interesting that this latter distribution looks as if it was centered on $\alpha \sim 0.7$ but got chopped by the JVAS/CLASS bias against steep sources. In this sense, is the newer data making the 154-source sample more physical, given the conventional radio galaxy knowledge?

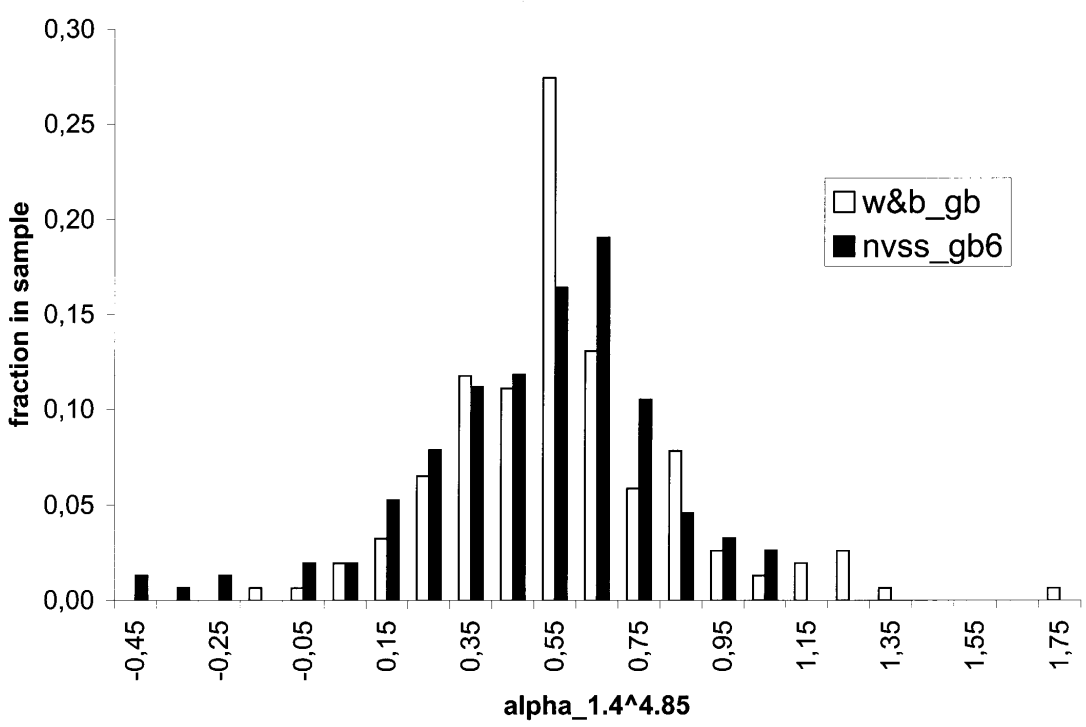

Figure B.1: *White:* The spectral index distribution ($\alpha_{1.4}^{4.85}$) of the 154-source sample constructed as in (Augusto et al. 1998) but regardless of the spectral index values of the sources (μ=0.57; s_{n-1} =0.28) — one source has no valid value so it was excluded. *Black:* Now the distribution is with the new values (two sources with no data were excluded) — it is skewed (μ=0.50; s_{n-1} =0.28).

Appendix C

55-source sample compactness at 5 GHz

Table C.1: In this table we present the ∼5 GHz flux densities of the 55 sources from GB6 and MERLIN (Augusto et al. 1998), which has a beam ∼ 1000 smaller than the GB6 survey. C is the compactness parameter for all sources determined from $(S_{GB6}-S_{MERLIN})/S_{GB6}$. Variability has to be small or non-existent for C to have any meaning. The more compact a source is, the closer to zero is C: core-dominated, $C = 0$; lobe-dominated, $C = 1$. 'neg' means that the value also turned out the other way around: likely truly variable sources.

Source (B1950.0)	S_{GB6} (mJy)	S_{MERLIN} (mJy)	C (B1950.0)	Source (mJy)	S_{GB6} (mJy)	S_{MERLIN}	C
0046+316	302	199	0.34	1150+095	432	401	0.07
0112+518	192	160	0.17	1211+334	627	795	neg
0116+319	1609	1279	0.21	1212+177	501	377	0.25
0127+145	570	455	0.20	1233+539	212	256	neg
0205+722	528	407	0.23	1241+735	312	175	0.44
0218+357	1480	—	—	1317+199	325	283	0.13
0225+187	155	140	0.10	1342+341	148	138	0.07
0233+434	243	190	0.22	1504+105	221	201	0.09
0345+085	207	113	0.45	1628+216	232	194	0.16
0351+389	208	117	0.44	1638+124	1207	993	0.18
0352+825	173	164	0.05	1642+053	363	265	0.27
0418+148	309	204	0.34	1722+562	125	182	neg
0429+174	300	261	0.13	1744+260	263	221	0.16
0529+013	162	152	0.06	1801+036	239	100	0.58
0638+357	212	193	0.09	1812+412	517	516	0.00
0732+237	493	526	neg	1857+630	160	146	0.09
0817+710	274	298	neg	1928+681	306	341	neg
0819+082	192	167	0.13	1947+677	—	—	—
0821+394	1031	—	—	2101+664	77	103	neg
0824+355	751	856	neg	2112+312	238	220	0.08
0831+557	5740	—	—	2150+124	290	215	0.26
0905+420	222	124	0.44	2151+174	220	191	0.13
0916+718	295	—	—	2201+044	653	254	0.61
1003+174	345	380	neg	2205+389	291	259	0.11
1010+287	323	268	0.17	2210+085	205	179	0.13
1011+496	299	331	neg	2247+140	1240	1235	0.00
1058+245	210	191	0.09	2345+113	228	173	0.24
1143+446	226	199	0.12				

Appendix D

55-source sample variability

Table D.1: In this table we present the flux density values at different frequencies *only* for the 21 sources that are 'variable': basically the ones that have data on the NASA Extragalactic Database (NED) *and* show variability as discussed in Section 3.1.4. We have yet to make the list of the other two types of sources from the 55-source sample: i) the ones for which NED has no data at all; ii) the ones for which NED has data at some frequencies but they do not seem to vary. We will build a table like the one here for such objects, also including observation dates. For the two sources marked (*), the variability is known not to be secular since these are well studied sources (one lens and one BL Lac). References: 1) NVSS; 2) (White & Becker 1992); 3) (Kühr et al. 1981); 4) WENSS; 5) GB6; 6) (Bennett et al. 1986); 7) (Pauliny-Toth et al. 1978); 8) (Owen et al. 1980); 9) (Zhang et al. 1997); 10) (Zhang et al. 1993); 11) (Becker et al. 1995); 12) 7C/6C (e.g. (Waldram et al. 1996)); 13) Parkes Catalogue (1990), Australia Telescope National Facility, Wright & Otrupcek, (Eds); 14) (Pauliny-Toth & Kellermann 1972); 15) (Griffith et al. 1995); 16) (Stull 1971); 17) (Kovalev et al. 1999); 18) JVAS (e.g. (Patnaik et al. 1992)); 19) FIRST (e.g. (Becker et al. 1995)).

Source	Freq. (GHz)	Flux density (mJy)	Ref.
B0112+518	1.4	448 ± 14	1
		$328 \pm 15\%$	2
B0116+319	0.318	3380 ± 150	3
		3941	4
B0127+145	5	570 ± 50	5
		662	6
B0205+722	1.4	670 ± 21	1
		$842 \pm 15\%$	2
B0218+357*	5	1480 ± 131	5
		1160 ± 10	7
	2.7	$1.14 \pm 0.06 \times 10^3$	8
		$1.03 \pm 0.02 \times 10^3$	3
	1.4	1708 ± 52	1
		$1456 \pm 15\%$	2
	0.318	2460	4
		1640 ± 160	3
B0429+174	5	395	6
		300 ± 27	5
B0817+710	1.4	$436 \pm 15\%$	2
		603 ± 19	1
B0819+082	5	114	6
		192 ± 17	5
B0916+718	1.4	$384 \pm 15\%$	2
		491 ± 18	1
B1010+287	1.4	$612 \pm 15\%$	2
		642 ± 20	1
		$566 \pm 5\%$	11
		621.82	19
B1211+334	1.4	1418	1
		$1196 \pm 15\%$	2
		1417.99	19
	0.151	$1.37 \pm 10\% \times 10^3$	12
		$1.69 \pm 0.05 \times 10^3$	12

Source	Freq. (GHz)	Flux density (mJy)	Ref.
B1212+177	5	320	13
		413	6
		501 ± 44	5
	1.4	$836 \pm 15\%$	2
		1011 ± 31	1
		1027.30	19
B1241+735	1.4	295 ± 11	1
		$218 \pm 15\%$	2
B1628+216	1.4	509 ± 16	1
		$300 \pm 15\%$	2
		482.86	19
B1638+124	5	1207 ± 107	5
		812	6
		1090	13
		$1.04 \pm 0.01 \times 10^3$	14
B1642+054	5	363 ± 32	5
		308 ± 19	15
		278	6
B1722+562	0.151	1230 ± 50	12
		920	12
B1801+036	1.4	274 ± 9	1
		$462 \pm 15\%$	2
B2201+044	8.4	$360 \pm 5\%$	18
		$0.45 \pm 7.7\% \times 10^3$	16
	5	653 ± 58	5
		530	13
	3.9	347 ± 115	3 ???
		508 ± 5	17
	2.7	800	13
		450 ± 100	3
	1.4	467 ± 17	1
		$784 \pm 15\%$	2
		1.0	13
B2205+389	1.4	553 ± 17	1
		$445 \pm 15\%$	2
B2210+085	5	205 ± 18	5
		153 ± 13	15

Appendix E

Searching for genuine one-sided CJs

This is a new part of the project, a bonus from our efforts of trying to understand the 55-source sample. The standard model of AGN, as described in (Augusto et al. 1999), predicts a supermassive black hole (SBH) feeding on galactic material which, in turn, is converted into powerful twin-sided radio jets emitted as far as 1 Mpc from the nucleus of the galactic host where the SBH lies. Indeed, there is overwhelming evidence for twin-sided radio sources, even in cases where detecting the weak 'counter-jet' has been difficult. However, it is not excluded the possibility that SBH can actually produce *intrinsic* one-sided radio jets. This situation is only physically understood, due to preservation of momentum, if the SBH is actually moving in the opposite direction of the jet as if propelled by it. What could these cases (even in small numbers) imply for the standard model of AGN? would these 'fast moving' SBH have any physical differences from the 'ordinary' SBH? what are the typical hosts of these 'flying beasts'?

(Saikia et al. 1996) address the possibility of existence of such sources within the framework of the standard model of AGN (by carefully examining one serious candidate). At the moment all existing candidates have arcsecond sizes. There is no reason, however, why we should not find candidates on sub-arcsecond scales: e.g. the 55-source sample. The facts are (Saikia et al. 1996): a typical radio galaxy with $\alpha \sim 0.8$, $v_{bulk}^{jet} \leq 0.6c$ and less than 45° inclined to the plane of the sky has jet/counter-jet flux density ratio less than 30 : 1. If this ratio is found to be much greater, then either its inclination angle is much larger than 45° (and unification does not work, since the radio galaxy should then 'turn' into a radio quasar) or it is an instrinsically one-sided source. Currently, there are no other alternatives.

The ideal wavelength for detecting the extended structure characteristic of radio jets (like blobs and knots) is L-band (1.4-1.6 GHz). We have now such maps available for a portion of our sample. As a preliminary study, we concentrate on the MERLIN L-band maps for 13 of the largest sources in our sample (Figure 2.4). In Table E.1 we show the jet/counter-jet flux density ratios for these sources, as well as their radio morphology (now as 'twin-sided vs. one-sided' as opposed to 'CSO/MSOs vs. CJs') and optical data. Five out of nine CJs are candidates. No CSO/MSOs is candidate (so far), as expected.

Of our five candidates, then, we must crucially locate their cores to be convinced that it is worth to do some further studies in any of them. The optical data that we are to analyse soon should tell us about the hosts of the five candidates and indicate if they are radio quasars (as it is likely) and hence beaming effects explain the large R, or if they are radio galaxies which,

Table E.1: In this table we present the jet/counter-jet flux density ratios (R) for the 13 sources of our sample observed with MERLIN at 1.6 GHz (Figure 2.4). On top we show the five candidate genuine one-sided radio sources ($R > 30:1$). Note that for these R is actually a lower limit. R- BSO: red-blue stellar object (POSS); EF: empty field; G: galaxy. *We do not really know where the core is for this object

Source	L-band morphology	Opt. Id. (V mag)	$\alpha_{1.4}^{4.85}$ (old/new)	R
B0351+390	one-sided	BSO (19.6)	$-0.14/-0.04$	$> 40:1$
B0821+394	one-sided?*	BSO (18.0)	0.25/0.29	$> 350:1$?
B0916+718	one-sided	BSO (18.5)	0.22/0.41	$> 75:1$
B1642+054	one-sided	EF	0.42/0.34	$> 32:1$
B2150+124	one-sided	BSO (19.5)	0.38/0.32	$> 64:1$
B0205+722	twin-sided	G (18.0)	0.33/0.19	$4:1$
B0429+174	one-sided	EF	0.37/0.18	$17:1$
B0824+355	twin-sided	QSO	0.12/0.20	$2:1$
B0831+557	one-sided	G (17.5)	0.24/0.30	$16:1$
B1011+496	one-sided	BSO (16.8)	0.24/0.19	$10:1$
B1241+735	one-sided	G (17.0)	$0.33/-0.05$	$16:1$
B1722+562	where is core?	BSO (19.8)	0.41/0.38	?
B2101+664	CSO?	RSO (18.0)	0.30/0.22	?

together with identifying their cores, would make them quite interesting for further study. Of course, it is important to quantify in how much the $\alpha < 0.5$ in our sources would indicate beaming effects as dominant, even if they all are radio galaxies. Ideally we should have $\alpha \sim 0.8$ radio galaxies as stated above. It is still surprising that we see blobs so close to the cores in one side and nothing at all in the other side. For any future follow up of strong cases, the VLA L-band is the ideal instrument since it can put very strong limits on R (or finally detect the counter-jet).

If we are successful we may tell a story about the size evolution of genuine one-sided sources, by comparing the results from our sample with the ones from VLBI and VLA surveys (smaller and larger scales, respectively).

Appendix F

Very inverted spectrum sources

This is yet another bonus. At the moment not more than a list of the sources picked from the parent sample that show very inverted radio spectra. These were actually chosen from a subsample of 820 sources (JVAS/CLASS) presented in (Augusto 1996) and used for statistical analysis. They are all point sources in the original VLA 8.4 GHz maps. Could they be bright objects at sub-mm wavelengths?

Table F.1: Very Inverted spectrum sources (with $\alpha < -1$). The 365 MHz flux densities come from the TEXAS survey (Douglas et al. 1996) and the 8.4 GHz (plus polarizations) from the JVAS (e.g. (Patnaik et al. 1992)).

Source	$\alpha_{1.4}^{4.85}$ (old/new)	$\alpha_{0.365}^{8.4}$	8.4 GHz polzn.	z	Opt. Id.	Comments
B0106+388	$-0.94/-0.92$	< -0.40	0.1%	0.7	Gal.	5 GHz GPS (Snellen et al. on it)
B0740+76	$-1.0/-1.2$				Gal.?	10 GHz GPS ?
B1005+066	$-0.94/0.01$	< -0.32	10%			5–10 GHz GPS
B1404+286	$-0.93/-0.85$	-0.76	0.7%	0.08	Gal.	well studied 6 GHz GPS
B1423+146	$-1.25/-0.45$	0.04	3%	0.78	QSO	5 GHz GPS
B1601+112	$-1.30/-0.93$	< -0.11	3%			5 GHz GPS
B2005+642	$-1.16/-0.26$			1.57	QSO	10 GHz GPS

Appendix G

The 100-object representatives of the parent sample (optical)

Table G.1: In this table we present the 100 objects randomly selected from the 1665-source parent sample to be studied in the optical and to be used as 'control' for the 55-source sample. Only 30 of the objects lack redshift information. Many have photometric information available in the literature.

Source (B1950.0)	R.A. (J2000.0)	Dec. (J2000.0)	z	Opt. id. POSS (other)	Photometry available	Comments
B0017+200	00 19 37.85446	20 21 45.5695		(20.0)	BVRI	blazar
B0017+257	00 19 39.78134	26 02 52.3448	0.284	(15.4)	BR + far IR	fairly known radio
J0034+390	00 34 01.60	39 00 20.9		EF		
J0044+393	00 44 35.90	39 19 35.0		EF		
B0106+013	01 08 38.7714	01 35 00.319	2.099	(18.3)	VR	well known
B0121+560	01 24 25.82647	56 18 51.9134		EF		
B0140+120	01 43 31.09319	12 15 42.9472		20.5		
B0158+031	02 00 40.81720	03 22 49.5016	0.765	(21.1)		
B0242+238	02 45 16.85714	24 05 35.1893		20.5		
B0251+393	02 54 42.63160	39 31 34.7140	0.289	(17.0)		
B0303+051	03 05 48.19157	05 23 31.5194		EF		
B0307+380	03 10 49.88050	38 14 53.8452	0.816	EF		
B0327+364	03 30 34.76550	36 39 41.0339		EF		
B0332+078	03 34 53.31830	08 00 14.4520		(21.5)		Stickel et al (on chase + Drinkwater)
B0353+289	03 56 8.46010	29 03 42.2768		19		
B0406+121	04 09 22.00919	12 17 39.8465	1.02	(20.5)	BVRIJHK	
B0420+022	04 22 52.21501	02 19 26.9364		20		
B0442+071	04 45 01.42928	07 15 53.9306		20.5		
B0514+109	05 16 46.64626	10 57 54.7726	(2.34?)	(18.0)		inconclusive redshift (Wills & Wills 76)
J0554+689	05 54 00.80	68 57 54.8		21		
B0612+570	06 17 16.92290	57 01 16.4162		18		
B0635+351	06 39 9.58868	35 06 22.5427		EF		
B0718+374	07 22 1.25998	37 22 28.6279		18		raw spectra: OHP 1.9m
B0735+674	07 40 53.39840	67 19 8.2271		20		
J0735+712	07 35 01.90	71 15 09.8	?	(17.4)		spectra: Lau et al 98 (no good)
B0740+173	07 43 05.10666	17 14 24.4050		19		
B0741+294	07 44 51.36551	29 20 6.0447	1.18	(15.9)		
J0800+489	08 00 33.80	48 54 12.9		EF		
B0805+010	08 08 04.34588	00 57 07.5817		19		
B0823+033	08 25 50.3387	03 09 24.519	0.506	(18.5)		well known (radio)
B0824+110	08 27 06.51335	10 52 24.1504	2.278	(18.5)	UBVR + far IR	well known
B0833+416	08 36 36.89322	41 25 54.7062	1.298	(17.2)		
B0839+187	08 42 05.09444	18 35 40.9875	1.27	(16.4)		fairly known (radio)
B0851+719	08 56 54.86951	71 46 23.8943		19		
B0854+213	08 56 57.24453	21 11 43.6442		20.5		
B0912+297	09 15 52.40015	29 33 23.9790	?	(16.0)	UBVRIHK	BLLac; bad spec. (Marcha et al 96); raw: OHP
J0917+737	09 17 29.20	73 43 00.9		EF		
B0922+407	09 26 0.42727	40 29 49.6727	1.876	(19.6)		
B0946+181	09 49 39.76272	17 52 49.4223	?	16		raw spectra: OHP 1.9m
B1004+141	10 07 41.49851	13 56 29.6010	2.707	(19.)	U + IR	
B1035+046	10 37 39.33991	04 24 01.7493		19.5		
J1035+557	10 35 44.40	55 42 51.8		EF		
B1042+178	10 45 14.36053	17 35 48.0876		21		
B1045+011	10 48 07.74540	00 55 43.4779		EF		
B1049+215	10 51 48.78950	21 19 52.3485	1.30	(18.5)		fairly known (radio)
B1055+018	10 58 29.6054	01 33 58.823	0.888	(18.3)	HJKL	very well studied (radio)
B1055+567	10 58 37.72617	56 28 11.1834	0.144?	(15.8)		z=0.144: Bade et al 98; z=0.41: Marcha et al 96
B1106+150	11 09 14.04395	14 44 52.9378		20.5		
B1111+149	11 13 58.6954	14 42 26.951	0.869	(18.)		
J1113+688	11 13 48.40	68 53 38.0		EF		
B1121+325	11 24 3.01102	32 14 14.0607		EF		
J1141+497	11 41 57.30	49 44 55.0		EF		
B1150+812	11 53 12.5	80 58 28	1.25	(18.5)		well known (radio)
J1151+589	11 51 25.10	58 59 30.8		EF		
B1204+124	12 07 12.62454	12 11 45.8846		20		
B1208+186	12 11 06.68635	18 20 34.2570		20		
B1212+171	12 15 03.97810	16 54 37.9356		20.5		on chase: Brinkman
B1222+438	12 24 51.50593	43 35 19.2815		18		

Source (B1950.0)	R.A. (J2000.0)	Dec. (J2000.0)	z	Opt. id. POSS (other)	Photometry available	Comments
B1226+638	12 29 6.02558	63 35 0.9862		(18.7)		
B1320+394	13 22 55.66151	39 12 7.9842	2.98	(17.)		
B1322+835	13 21 45.0	83 16 06		18.5		on chase: Stickel
B1331+094	13 34 19.56240	09 12 00.3655		21		
B1401+000	14 04 12.12424	-00 13 25.1293		19.5		
B1413+373	14 15 28.46657	37 06 21.1789	2.36	(18.)		
B1421+048	14 24 09.50169	04 34 52.0587		(18.0)		
B1421+482	14 23 6.15619	48 02 10.8466	2.22	(18.9)		
B1424+240	14 27 0.39510	23 48 0.0410	?	16	VRI	featureless spectra (Marcha 95); well known
B1428+422	14 30 23.74175	42 04 36.5027	4.715	EF(20.9)		3rd fartest QSO!
B1433+304	14 35 35.40150	30 12 24.5284		EF		
B1436+373	14 38 53.61102	37 10 35.4244		20		
B1509+348	15 11 20.10480	34 39 32.6621		EF (22.5)		
J1534+586	15 34 56.30	58 39 28.8	1.895	(19.)		
B1546+027	15 49 29.4371	02 37 01.164	0.413	(18.)	vgr	very well studied (radio)
B1607+563	16 08 20.75183	56 13 56.3728		18.5		
B1642+690	16 42 7.84860	68 56 39.7580	0.751	(19.2)	far IR	very well studied (radio)
B1643+113	16 45 54.67508	11 13 52.6366		EF		
B1657+265	16 59 24.14917	26 29 37.0184	0.795	(18.)		
B1726+552	17 27 23.46926	55 10 53.5449		18		
J1727+587	17 27 32.40	58 46 29.0		19.5		
B1746+197	17 49 05.47453	19 44 08.8515		17.5		
B1749+096	17 51 32.81889	09 39 00.7306	0.322	(16.8)	VRIJHK	well studied
B1752+356	17 54 13.67609	35 40 48.5488	0.55	17.5		QSO
J1757+479	17 57 28.40	47 57 30.9		EF		
B1803+784	18 00 45.6	78 28 03	0.68	(17.)	JHK+12-100u IRAS	very well studied (radio)
B1807+279	18 09 11.97952	27 58 11.8073	1.76	(17.5)		
B1825+269	18 27 55.42709	26 58 5.9228		20.5		
J1841+676	18 41 42.20	67 40 07.9		EF		
B1846+322	18 48 22.09068	32 19 2.5472		19.5		on chase: Brinkman
B1850+402	18 52 30.37400	40 19 6.6006	2.12	(18.5)		
J1903+515	19 03 12.10	51 30 42.9		EF		
B1926+611	19 27 30.44283	61 17 32.8767		18		on chase: Stickel
B1950+573	19 51 6.98368	57 27 17.1945	0.652	(18.0)		
B2007+777	20 05 30.9	77 52 43	0.342	(16.5)		BLLac; very well studied (radio)
B2015+083	20 18 11.31215	08 31 54.5533		EF		
B2049+175	20 51 35.58342	17 43 36.9145		19		
B2051+687	20 52 0.24770	68 58 15.7320		20		
B2112+283	21 14 58.33397	28 32 57.2055				
B2358+189	00 01 08.62256	19 14 33.8160	3.10	(20.5)		

Appendix H

Double-double radio galaxies

(Schoenmakers et al. 2000) have recently proposed this new type of radio source. Although they discuss Mpc-scale radio galaxies, can we apply the same definition to our much smaller (and younger) objects? will the properties of smaller versions be similar?

From our sample (images in (Augusto et al. 1998; Augusto et al. 1999) and Figure 2.4), we have one (obvious) source that could be candidate to such a morphology: B1801+036. Others may be hidden under the yet to classify radio structure.

References

Allington-Smith J. R., Spinrad H., Djorgovski S., Liebert J., 1998, MNRAS, 234, 1091

Antonnucci R. R. J., 1985, ApJS, 59, 499

Augusto P., Wilkinson P. N., Browne I. W. A., 1998, MNRAS, 299, 1159

Augusto P., Gonzalez-Serrano J. I., Edge A. C., Gizani N. A. B., Perez-Fournon I., 1999, in Documento FCT - Julho 99 (dossier of ESO Project proposed)

Augusto P., 1996, Ph.D. Thesis, University of Manchester, UK

Bade N., Beckmann V., Douglas N. G., Barthel P. D., Engels D., Cordis L., Nass P., W. V., 1998, A&A, 334, 459

Becker R. H., White R. L., Helfand D. J., 1995, ApJ, 450, 559

Bennett C. L., Lawrence C. R., Burke B. F., Hewitt J. N., Mahoney J., 1986, ApJS, 61, 1

Browne I. W. A., Patnaik A. R., Walsh D., Wilkinson P. N., 1993, MNRAS, 263, L32

Browne I. W. A., Patnaik A. R., Wilkinson P. N., Wrobel J. M., 1998, MNRAS, 293, 257

Bugaenko O. I., Gorshkov A. G., Esipov V. F., Konnikova V. K., Novikov S. B., 1993, Ast. Let., 19, 5

Bursov N. N., 1997, Astron. Rep., 41, 35

Capetti A., Axon D. J., Macchetto F., Sparks W. B., Boksenberg A., 1996, ApJ, 469, 554

Cid Fernandes R., Storchi-Bergmann T., Schmitt H. R., 1998, MNRAS, 297, 579

Condon J. J., Cotton W. D., Greisen E. W., Yin Q. F., Perley R. A., Taylor G. B., Broderick J. J., 1998, AJ, 115, 1693 (NVSS)

Crawford C. S., Allen S. W., Ebeling H., Edge A. C., Fabian A. C., 1999, MNRAS, 306, 857

de Bruyn A. G., Sargent W. L. W., 1978, AJ, 83, 1257

Douglas J. N., Bash F. N., Bozyan F. A., Torrence G. W., Wolfe C., 1996, AJ, 111, 1945

Falco E. E., Kochanek C. S., Muñoz J. A., 1998, ApJ, 494, 47

Fletcher A., et al., 1996, Astron. Rep., 40, 759

Foltz C. B., Weymann R. J., Peterson B. M., Sun L., Malkan M. A., Chaffee F. H., 1986, ApJ, 307, 504

Gelderman R., Whittle M., 1994, ApJS, 91, 491

Geldzahler B. J., Witzel A., 1981, AJ, 86, 1306

Genzel R., Pauliny-Toth I. I. K., Preuss E., Witzel A., 1976, AJ, 81, 1084

Gower J. F. R., Scott P. F., Wills D., 1965, MmRAS, 69, 183

Gregorini L., Vigotti M., Mack K.-H., Zonnchen J., Klein U., 1998, A&AS, 133, 129

Gregory P. C., Condon J. J., 1991, ApJS, 75, 1011

Gregory P. C., Scott W. K., Douglas K., Condon J. J., 1996, ApJS, 103, 427 (GB6)

Griffith M. R., Wright A. E., Burke B. F., Ekers R. D., 1995, ApJS, 97, 347

Henstock D. R., Browne I. W. A., Wilkinson P. N., McMahon R. G., 1997, MNRAS, 290, 380

Hook I. M., McMahon R. G., Irwin M. J., Hazard C., 1996, MNRAS, 282, 1274

Joyce R. R., Simon M., 1976, PASP, 88, 870

Koski A. T., 1978, ApJ, 223, 56

Kovalev Y. Y., Nizhelsky N. A., Kovalev Y. A., Berlin A. B., Zhekanis G. V., Mingaliev M. G., Bogdantsov A. V., 1999, A&AS, 139, 545

Kühr H., Witzel A., Pauliny-Toth I. I. K., Nauber U., 1981, A&AS, 45, 367

Large M. I., Mills B. Y., Little A. G., Crawford D. F., Sutton J. M., 1981, MNRAS, 194, 693

Laurent-Muehleisen S. A., Kollgaard R. I., Moellenbrock G. A., Feigelson E. D., 1993, AJ, 106, 875

Laurent-Muehleisen S. A., Kollgaard R. I., Ciardullo R., Feigelson E. D., Brinkmann W., Siebert J., 1998, ApJS, 118, 127

Lawrence C. R., 1996, in Kochanek C., Hewitt J. N., eds, "Astrophysical Applications of Gravitational Lensing", IAU Symposium nr. 173. Kluwer Academic Publishers, p. 299

Le Borgne J.-F., Mathez G., Mellier Y., Pelló R., Sanahuja B., Soucail G., 1991, A&AS, 88, 133

Machalski J., 1991, Acta Astron., 41, 39

Marcha M. J. M., Browne I. W. A., Impey C. D., Smith P. S., 1996, MNRAS, 281, 425

Marcha M. J. M., 1995, Ph.D. Thesis, University of Manchester, UK

Owen F. N., Porcas R. W., Mufson S. L., Moffett T. J., 1978, AJ, 83, 685

Owen F. N., Spangler S. R., Cotton W. D., 1980, AJ, 85, 351

Patnaik A. R., Browne I. W. A., Wilkinson P. N., Wrobel J. M., 1992, MNRAS, 254, 655

Patnaik A. R., Browne I. W. A., King L. J., Muxlow T. W. B., Walsh D., Wilkinson P. N., 1993, MNRAS, 261, 435

Paturel G., Petit C., Prugniel P., Garnier R., 1999, A&AS, 140, 89

Pauliny-Toth I. I. K., Kellermann K. I., 1972, AJ, 77, 797

Pauliny-Toth I. I. K., Witzel A., Preuss A., Kuhr H., Kellermann K. I., Fomalont E. B., Davis M. M., 1978, AJ, 83, 451

Rees N., 1990, MNRAS, 244, 233

Rengelink R. B., Tang Y., de Bruyn A. G., Miley G. K., Bremer M. N., Roettgering H. J. A., Bremer M. A. R., 1997, A&AS, 124, 259 (WENSS)

Saikia D. J., Thomasson P., Jackson N., Salter C. J., Junor W., 1996, MNRAS, 282, 837

Scarpa R., Urry C. M., Falomo R., Treves A., 1999, ApJ, 526, 643

Schoenmakers A. P., de Bruyn A. G., Röttgering H. J. A., van der Laan H., Kaiser C. R., 2000, MNRAS, 315, 371

Shimmins A. J., Wall J. V., 1973, Au. J. Ph., 26, 93

Smail I., 2000, Ian Smail — http://star- www.dur.ac.uk/ irs/images/a2390vi.gif

Soboleva N. S., Pariiskii Y. N., Naugol'naya M. N., 1994, Astron. Rep., 38, 605

Spencer R. E., McDowell J. C., Charlesworth M., Fanti C., Parma P., Peacock J. A., 1989, MNRAS, 240, 657

Stickel M., Kühr H., 1996, A&AS, 115, 1

Stickel M., Rieke G. H., Kühr H., Rieke M. J., 1996, ApJ, 468, 556

Stull M. A., 1971, AJ, 76, 1

Tran H. D., 1985, ApJ, 440, 578

Vermeulen R. C., Taylor G. B., Readhead A. C. S., Browne I. W. A., 1996, AJ, 111, 1013

Veron-Cetty M.-P., Veron P., 1993, A&AS, 100, 521

Waldram E. M., Yates J. A., Riley J. M., Warner P. J., 1996, MNRAS, 282, 779 (7C/6C)

White R. L., Becker R. H., 1992, ApJS, 79, 331

Whyborn N. D., Browne I. W. A., Wilkinson P. N., Porcas R. W., Spinrad H., 1985, MNRAS, 214, 55

Wills D., Wills B. J., 1976, ApJS, 31, 143

Zhang X., Zhen Y., Chen H., Wang S., 1993, A&AS, 99, 545

Zhang X., Zheng Y., Chen H., Wang S., Cao A., Peng B., Nan R., 1997, A&AS, 121, 59